Power Allocation in Energy Harvesting Two-way Relay Systems

by

Lingqian Zeng

A Thesis Submitted in Partial Fulfillment

of the Requirements for the Degree of

Master of Applied Science

in

The Department of Electrical, Computer, and Software Engineering

University of Ontario Institute of Technology

April 2015

Contents

List of Tables

List of Figures

Abstract

In this thesis, we consider two-way relaying in a wireless communication system with two transceivers and one relay node. In such a model, two scenarios are taken into account: a system with one energy harvesting (EH) relay node and a system with two EH transceivers and one EH relay node. Under these two assumptions, we study the optimization problem of harvesting energy allocation which maximizes the total data throughput of a wireless network under some restrictions at the EH node(s).

In the first scenario, only the relay node is powered up by the harvested energy and the other two transceiver nodes are powered up by conventional power supply. We first find that the data transmission rate of the system monotonically increases and is strictly concave in the power of the relay. As a result, we can obtain an optimal power control policy of the relay for maximizing the total throughput. This optimization problem can be solved not only by conventional optimization solvers, but also by a method called breaking-rope. Finally, we propose a novel algorithm to solve the optimization problem based on the breaking-rope.

For the case of system with three EH nodes, the problem is more complicated since multiple optimization parameters, which are the transmitting power of three EH nodes, should be taken into account. Because the objective function is not jointly concave in all three parameters, it is difficult to find a feasible solution. Hence, we have to simplify the objective function to overcome the difficulty in solving the original problem. By relaxing the problem, we aim to find the upper bound of the total throughput. It is shown that the upper bound function is concave in one parameter

when other two parameters are fixed. Thus, the optimal solution can be obtained by using the iterative Alternate Convex Search method.

The performance of the proposed schemes are evaluated by computer simulations. The breaking-rope method is capable of acquiring the optimum policy in the one EH node system. For the three EH node system, we show that our solution based on the Alternate Convex Search method performs closely to the best-case and outperforms the breaking-rope method.

Acknowledgements

I would like to express my gratitude to my supervisor Dr. Shahram Shahbazpanahi for all his excellent guidance, patience, and motivation. Dr. Shahbazpanahi has been always ready to support and direct me. He helped me in establishing the research skills.

I am grateful to my parents and my sister for their love. They were always supporting me and encouraging me with their best wishes.

I would also like to thank all my friends and colleagues whose support, reviews, insights, and company will always be remembered.

Oshawa, Ontario — Lingqian Zeng

September 12, 2015.

Chapter 1

Introduction

1.1 Overview

Over the past decades, wireless communication has experienced remarkable development. The rapidly growing demands for wireless services have resulted in strict requirements for wireless devices. One of the requirements focuses on the power supply for wireless devices that plays a significant role in wireless communication. Conventional non-rechargeable batteries have been replaced by rechargeable batteries which have gained increasing popularity in the industry. However, normal rechargeable batteries mainly rely on cables or power grids to gain electricity, and thus, cannot satisfy the task of working in remote areas, such as mountains, desert, or underwater. These extreme working conditions have brought great challenges to the design of wireless devices with conventional rechargeable batteries. Furthermore, due to the scarcity of natural resources and the carbon dioxide released by fuel burning, the utilization of renewable energy has become an urgent requirement in the industry. Thus, how to obtain green energy, and how to efficiently use energy has attracted the interest of researcher. As a consequence, rechargeable batteries equipped with an energy harvesting technique have emerged in response to current needs.

Energy harvesting (EH) is a technique by which energy is derived from ambient sources and stored in rechargeable batteries for the purpose of powering up small wireless devices. Wireless devices equipped with a suitable EH component are expected to break the limitation of power grids and are capable of operating in areas with no power facilities. Moreover, the energy generated by EH technique is green and environmentally friendly. The idea of harvesting renewable energy from ambient environments also reduces the costs of battery charging and cablecasting. Hence, the utilization of EH technique in wireless networks not only provides convenient and sustainable energy sources, but also expands wireless network coverage and reduces construction costs.

Nevertheless, the replacement of the traditional battery has an effect on the way we transmit data in a wireless network. In conventional wireless networks, non-rechargeable batteries can provide stable power for devices to ensure the system operates effectively. Although the harvested energy in an EH system can be virtually infinite, the amount of the harvested energy is sometimes unpredictable. Since the amount of harvested energy is random, there is no guarantee of sufficient energy stored in the battery at any moment. For instance, once the energy has been harvested and stored in the battery, it can be immediately used by the device. For this case, there is a trade-off between using the energy as soon as it is harvested and reserving the energy for the purpose of contingency. Hence, a scheme that is concerned about system performance and energy efficiency should be designed to guarantee the satisfaction of user requirements. Consequently, wireless network systems that rely on EH sources have to be designed from an EH point of view, both from a the hardware and software perspective [3].

Relaying techniques are introduced in order to overcome the problem of channel fading and to guarantee quality of transmission. In this thesis, we work on a two-way relay wireless communication system which adopts the EH technique in order to power up the transmitting nodes in the network. Given the transmission duration, we consider the total throughput maximization problem. Two different problems are studied, as discussed below:

- In the first problem, the two-way relay wireless network consists of two transceivers, which are powered up by conventional batteries, and one relay node, which is powered up by an EH unit. The total throughput of this model is a function of the transmitting power of the relay and is limited by two sets of constraints, namely energy causality constraints and battery capacity constraints.

- In the second problem, we study a network where the two transceivers and a relay are all EH nodes. This time, the total throughput is a function of the transmitting powers of three nodes. Specifically, each node has its own energy causality and battery capacity constraints. We aim to maximize the total throughput by jointly optimizing the transmitting powers in three nodes, subject to the constraints in each node.

The outline of this chapter is organized as follows: in the first section, we briefly explain the concept of energy harvesting, and then various harvested energy sources and techniques are introduced. In Section 1.2, the relay network techniques, along with different types of relaying schemes, are reviewed. Following that, the motivation and objectives of this thesis are presented. The last two sections present methodology and thesis organization.

1.2 Energy Harvesting Techniques and Sources

In recent decade, EH techniques have emerged as a promising research area which is rapidly developing to satisfy the power demands of low-power-consumption devices. Energy harvesting is the process of transferring other types of passive energy from the surrounding environment into electrical power [4]. The application prospects of such techniques are already vast. In addition to the widely-used distributed wireless sensor nodes, a wide range of applications have benefited from energy harvesting, such as wearable devices, unmanned vehicles, and military reconnaissance [5]. The harvestable energy sources can be light, solar, vibration, differences in temperature across a material, or even radio frequency (RF) signals in the air. In the following section, we will introduce different types of energy resources which can be used for energy harvesting.

1.2.1 Solar Energy

As we know, the sun is the most powerful energy source in the nature, and hence the techniques of transferring solar energy into electrical energy have attracted research interest for many years. At the earth's equator, on average 1000 W amount of solar energy hits a square meter of the earth's surface. This number may be changed at different geographical locations, but still shows an immense amount of potential of solar power. The most widely-used technique for collecting solar energy is based on a particular material which is called photovoltaic (PV) material. PV materials are capable of converting light energy directly into electrical energy by photovoltaic effect, which is a physical and chemical phenomenon.

Solar energy applications are very common in our every-day life and industry, including toys, watches, calculators, street lighting controls, portable power supplies, and satellites. Among these applications, solar cells are used to charge batteries and super capacitors to provide a stable energy source.

However, solar energy tends to be intermittent, and thus, is not available at all-times or in all-terrains since it can only be harvested in outdoor areas during the daytime. For example, a portable device which is designed to monitor an indoor patient's medical condition, throughout 24 hours, cannot be powered up by solar energy. Furthermore, the availability of daylight, cloud density, and the level of operation latitude, all profoundly influence the harvesting process. Thus, systems which rely on solar power are subject to location considerations.

1.2.2 Mechanical Vibration

Mechanical vibration is another rich resource which can be captured and transferred into electrical energy. The vibration, which is created by the movement of an object, can be converted to electrical energy through three methods: piezoelectric technique, electrostatic method, and electromagnetic technique [6].

In reality, the piezoelectric technique is the most convenient and efficient method. On average, piezoelectric material can harvest 35.4 mJ/cm^3 energy compared with electrostatic at 24.8 mJ/cm^3 and electromagnetic at 4 mJ/cm^3. Piezoelectric materials obtain mechanical vibration from pressures, vibrations, or force, and then convert them into electricity. These specific characteristics endow them with the ability to generate electrical charge when a mechanical load is applied.

As one of the vibration sources, everyday human actions such as body movements, breathing, blood pressure or footfalls, can generate power and become a source for energy harvesting. For example, researchers at the University of Michigan have developed a device that harvests energy from the reverberation of heartbeats through the chest and converts it to electricity to run a pacemaker or an implanted defibrillator. Table 1.1 tabulates the characteristics of different human vibration types and compares them with solar energy sources [1]. With the rise of wearable devices, including electronic wristbands, electronic watches, and electronic glasses, human activity has become a promising potential source to power these devices since conventional batteries add size, weight, and this presents inconvenience to present-day devices. As a result in future, this technique, which has the ability to transfer human activity into electricity, will definitely become increasingly common in wireless devices.

1.2.3 Radio Frequency Energy

The upsurge of wireless telecommunication enriches the radio environment, and thus motivates researchers to think about exploiting these abundant radio frequency

Table 1.1: Characteristic of Different Harvesting Energy Sources [1, 2]

Energy Sources	Characteristic	Availability of Energy	Conversion Efficiency	Amount of Energy Harvested
Solar	Ambient Uncontrollable Predictable	100 mW/cm^2	15 %	15 mW/cm^2
Footfalls	Fully controllable	67 W	7.5 %	5 W
Breathing	Unpredictable Uncontrollable	0.83 W	50 %	0.42 W
Blood Pressures	Unpredictable Uncontrollable	0.93 W	40 %	0.37 W

resources. The technique of radio frequency energy harvesting, or RF harvesting in short, is such a product. RF harvesting has emerged as an environmentally friendly approach in green communication and forms a promising alternative to existing energy resources. RF techniques convert radio frequency into direct currents by a receiving antenna and a converting circuit. The radio signals received by the antenna act as a medium to carry energy in the form of electromagnetic radiation with a frequency bandwidth ranging from 300 GHz to as low as 3 kHz [7], including TV, FM radio, mobile phone and Wi-Fi signals. After capturing the signals, the converting circuit processes and converts them into direct currents.

The RF energy harvesting technique explores a new way for communication systems to draw energy from the radio environment which is created by the wireless communication itself. Such an energy recycle attracts more and more interests in the energy harvesting field. The sustainable power supplied by the radio environment can break the lifetime limitation of conventional wireless networks where the major concerns are battery lifetime and replacement. Therefore, the RF energy harvesting techniques provide a promising scheme for energy-limited wireless networks. One of the current applications for wireless devices is battery-free wireless sensor which is applied in industrial monitoring, building automation, smart grid and agriculture. Moreover, in biomedical applications, RF is already being used experimentally to recharge the batteries in pacemakers and implanted transcutaneous electrical nerve stimulation devices.

1.3 Relay Networks in Wireless Communication

Most traditional wireless communication networks are based on a point-to-point communication structure in which a transmitter directly communicates with a receiver. The disadvantages of traditional wireless communication networks are quite obvious; e.g., relatively weak signal strength, relatively short-distance communication, and serious channel fading. All these issues result in transmitting power loss and poor transmission quality. To solve these problems, relay networks were created and became attractive for wireless communication communities [8, 9, 10].

Relay networks constitute a broad class of network topologies where a transmitter and a receiver are interconnected by means of one or more intermediate nodes. In such a network, the transmitter can hardly communicate with the receiver directly due to the poor quality of the channel between them. For this reason, two transceivers can exchange information with the help of the relay nodes. Different types of relay networks include one-way and two-way relaying schemes. Specifically, the two-way relaying scheme has attracted great attention in the wireless network design due to its bandwidth efficiency.

A two-way communication channel was first proposed by Shannon, showing how to design an efficient message exchange model to enable simultaneous bidirectional communication at the highest possible data rate [11]. The so-called bidirectional property means a node not only can be a transmitter, but also a receiver. Following Shannon's two-way communication structure, researchers introduced an additional relay to support the exchange of information between the two transceivers. This two-way relaying scheme can overcome the self-interference in the transceivers and provide additional spectral efficiency. There are three relaying protocols for the bidirectional relay channel with half-duplex nodes: the four-time-slot scheme, the time division

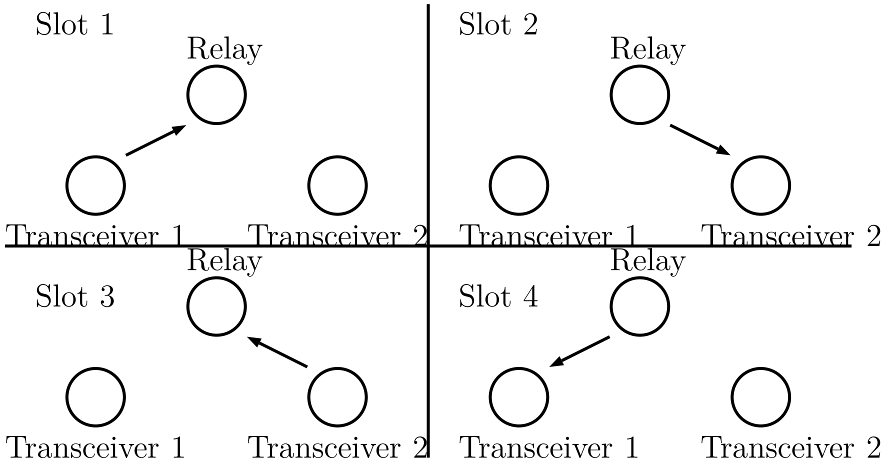

Figure 1.1: Four time-slot protocol of two-way relay

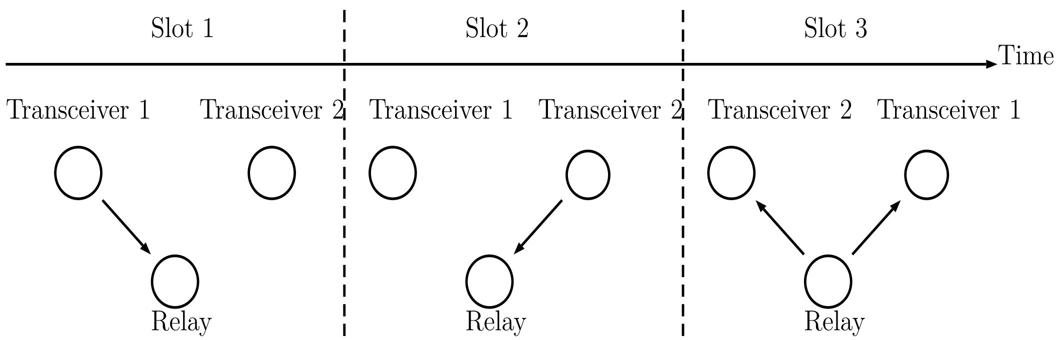

Figure 1.2: TDBC protocol of two-way relay

broadcast (TDBC), and the multiple access broadcast (MABC). These three protocols differ in the number of steps for message exchange.

In the four-time-slot scheme, two one-way relaying schemes are conducted in sequence to materialize the information exchange in two directions. The procedure is depicted in Figure 1.1. In Phase 1, Transceiver 1 transmits the signal to the relay and in Phase 2, the relay forwards the received signal to Transceiver 2. In phase 3, Transceiver 2 transmits its signal to the relay, and in Phase 4, the relay retransmits its received signal from Transceiver 2 to Transceiver 1.

The TDBC scheme takes three steps to exchange information between the two transceivers. The transmission process is shown in Figure 1.2. In the first step, Transceiver 1 transmits its own signal to the relay, and at the second slot, Transceiver 2 sends its own message to the relay. In the third slot, the signals, received from

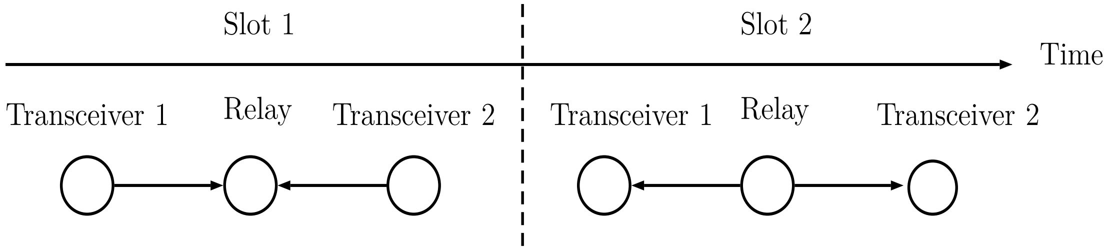

Figure 1.3: MABC protocol of two-way relay

Transceivers 1 and 2 at the relay, are combined and retransmitted to Transceivers 1 and 2.

The MABC protocol requires two steps to exchange information between the two transceivers. The procedure is illustrated in Figure 1.3. In the first phase, both Transceivers 1 and 2 simultaneously transmit their respective signals to the relay. In Phase 2, the relay transmits back an amplified and phase-adjusted version of the signals received from Transceivers 1 and 2.

Under each of the MABC and TDBC protocols, several relaying schemes are available based on various signal processing methods. Amplify and forward (AF), decode and forward (DF), and compress and forward (CF) are among the most popular relaying schemes [12]. These schemes are introduced as follows:

- *Amplify and forward*: The relay amplifies its received signal and directly retransmits the amplified signal to the receiver. The AF scheme requires no computation but carries the noise incurred in the first stage.

- *Decode and forward*: The relay decodes both messages from both transceivers before re-encoding them for transmission. The DF scheme requires the full codebooks of both users and a large amount of computation at the relay.

- *Compress and forward*: The relay compresses the received signal, and then reencodes and transmits the compressed signal. To do so, the relay requires the channel output distribution at the relay rather than the full codebooks.

1.4 Optimization Problem in an EH Half-Duplex Communication System

Investigations in the EH communication system mainly focus on two optimization problems: minimizing the transmission completion time given a certain amount of data; and maximizing the total throughput within a known deadline. These two problems are solved by obtaining the optimal power allocation(s) of the EH node(s). However, the power allocation of the EH node is subject to two constraints: energy causality and battery capacity. The energy causality constraint (also known as the energy constraint) stipulates that the energy cannot be used until it is harvested, and the battery capacity constraint confines the amount of energy stored in the battery. In this thesis, we study the throughput maximization problem in an off-line half-duplex EH communication system.

In the off-line setting, all energy harvesting profiles of the EH nodes, as well as all the channel state information are assumed to be known at the beginning of the transmission. Specifically, the energy harvesting profiles contain the arrival time and the amount of every harvested energy packet. In contrast, in an on-line setting case, only the past and current information of energy profiles and the channel state information are available.

A two-way communication system, which allows two users to communicate in both directions, can be categorized as full-duplex and half-duplex. In a full-duplex system, a user can simultaneously receive and transmit signals. For example, the telephone is an application of a full-duplex system. However, in a half-duplex system, a user can only transmit or receive signals at the one time; i.e., user A transmits while user B receives, or user B transmits while user A receives. An example of a half-duplex device is a walkie-talkie which has a “push-to-talk” button.

1.5 Motivation

As mentioned earlier, the need for green wireless communication devices is growing and this requires a wide range of wireless communication models using the EH technique. How to utilize the harvested energy in a most efficient way to satisfy user requirement has become a challenge for researchers. Moreover, the EH system models, which rely on various relaying strategies or different system settings, vary from case to case. Many specific models await examination from the aspect of both mathematical research and structural property observation. Current investigations in this field mainly focus on point-to-point and one-way relay systems. However, due to the bidirectional nature of communication, a two-way relaying scheme has its own merit in wireless communication. Only a few publications are concerned with a two-way relay EH system [11, 13, 14, 15, 16]. The scarcity of research on two-way relay EH systems which are bandwidth efficient motivates us to consider such a system in the wireless communication network.

1.6 Objective

We focus our study on signal processing aspects of EH systems instead of how to obtain the harvested energy. We consider the throughput maximization problem in an MABC-based two-way AF relaying half-duplex system with EH node(s). We also assume an off-line setting in which the harvested energy profiles and channel state information are known to us non-causally. We summarize the objectives of this thesis as listed below:

- In the case of one EH relay node, the main objective is to solve the total throughput maximization problem by optimizing the transmitting power of the relay node. We also impose the energy causality and battery capacity constraints on the relay's transmitting power for this optimization problem.

- The second objective is to maximize the total throughput of the network which consists of two EH transceivers and one EH relay node. In this three EH node case, the total throughput is maximized over the transmitting power of three EH nodes and subject to the energy causality and battery capacity constraints in each EH node.

1.7 Methodology

In this section, we briefly introduce our methodology toward the aforementioned problems.

- Our approach toward solving the first problem is based on the concavity of the objective function. We prove that the optimal relay power has certain properties which enable us to derive an algorithm to solve the throughput maximization problem.

- In the second problem, we encounter difficulty in solving the throughput maximization problem with the three optimization parameters which are the transmitting power of the three EH nodes. The objective function is not jointly concave in these three parameters, and thus, may not be amenable to a computationally affordable solution. A relaxed objective function has been proposed which aims to find the upper bound of the total throughput.

- To solve the upper bound optimization problem, we first break this problem into three sub-problems. For each sub-problem, we fix two parameters and search the optimal solution for the third parameter. By doing this, the sub-problem is concave in that third parameter and can be solved by any convex optimization method. We then iteratively solve these sub-problems until the solution converges to the optimum.

1.8 Thesis Organization

In Chapter 2, we conduct a literature survey on different types of EH systems in the relevant fields. In Chapter 3, the optimal relay power allocation for maximizing the total throughput in an two-way relay model with an EH relay node is studied. An algorithm is developed to solve the optimization problem. In Chapter 4, a system, consisting of three EH nodes, is introduced. We aim to maximize the total throughout of the network over the power in three EH nodes and subject to the battery and energy constraints. However, this problem is difficult to solve. After some mathematical manipulations, we devise a relaxed objective function which aims to obtain the upper bound of the total throughput. The Alternate Convex Search method is applied to tackle the upper bound problem by respectively optimizing the energy policies in the three nodes. The conclusions and future work are presented in Chapter 5.

Chapter 2

Literature Review

During the past few years, the volume of literature on energy harvesting communication systems has increased. Research has focused on obtaining the optimal data transmission policies under different assumptions. These assumptions concern the condition of battery capacity, the number of EH nodes in the wireless network, and the availability of knowledge about harvested energy. Among these publications, two optimization problems are mainly studied in the literature: maximizing the total throughput of a network by a certain deadline; and minimizing the transmitting completion time for a known amount of data. In this chapter, after briefly introducing the convex optimization problem, we present a literature review, which is categorized by the number of EH nodes in the system.

2.1 Convex Optimization Problem

A convex optimization problem is referred to an optimization problem where the objective function is a convex function, and the constraint set is a convex set[17]. The convex optimization problem is in the form of [18]

$$
\begin{aligned}
\text{minimize} \quad & f_0(x) \\
\text{s.t.} \quad & f_i(x) \le b_i, \quad i = 1, \cdots, m,
\end{aligned} \tag{2.1}
$$

where the functions $f_0, \cdots, f_m : \mathbb{R}^n \to \mathbb{R}$ are convex, i.e., satisfy

$$
f_i(\alpha x + \beta y) \le \alpha f_i(x) + \beta f_i(y)
$$

for all x, $y \in \mathbb{R}^n$ and all α, $\beta \in \mathbb{R}$ with $\alpha + \beta = 1$, $\alpha \ge 0$, $\beta \ge 0$.

In general, there may not be analytical formula for solving a given convex optimization problems, but many efficient methods have been developed to these problems. For example, interior-point methods work very well in reality.

2.2 Systems with One Energy Harvesting Node

A communication system with one EH node is widely considered in the literature for its simplicity. In such a system, either of the transceiver nodes or relay node can be powered up by EH devices. Moreover, different settings are considered for different scenarios.

2.2.1 Point-to-Point Systems

One of the first attempts to analyze an energy harvesting communication system from an information-theoretic perspective is in [19]. The authors focus on a point-to-point communication system in an additive white Gaussian noise (AWGN) channel with an EH transmitter. It is shown that the capacity of AWGN channel under energy harvesting consideration is identical to the capacity of the AWGN channel, where the average power of the entire codeword is limited by the average recharge rate of the harvested energy. In this paper, the authors also propose two schemes: the save-and-transmit and the best-effort-transmit schemes to achieve the upper bound of the channel capacity. This significant solution of the capacity in the AWGN channel provides a theoretical basis to the subsequent work.

In [20, 21, 22, 23], the authors consider a single-user continuous-time EH system. In such a system, the harvested energy can be stored in a battery and then is supplied to the transmitter during the transmission. In [21, 22], the battery capacity is assumed to be infinite. Although this assumption may not be practical in reality, the result can provide a benchmark for future study. [22] investigates two different scenarios. In the first scenario, all the data packets arrive before transmitting. In the second scenario, the data packets may arrive during transmission. By analyzing the structural properties of the optimal policy, two algorithms are proposed for obtaining the global optimal off-line energy allocation in these cases.

However, the battery capacity is assumed to be finite in [20, 23]. In [20], the authors rely on the concavity of the fairly common power-rate function [22], and first prove several necessary properties of the optimal policy in a throughput maximization problem. Based on these observations, an algorithm, which is used to solve the problem of data transfer in [24], can be used for obtaining an optimal solution in the energy transfer case. The authors also claim that the solution of the transmission completion time minimization problem is closely related to the throughput maximization problem. Therefore, the authors solve the completion time minimization problem through an algorithm which is derived under the same philosophy as the throughput maximization problem.

In [23], two methods are proposed to obtain the optimal energy allocation problem in both on-line and off-line settings. For an off-line setting, the authors first consider a throughput maximization problem in a static channel. They apply the Karush-Kuhn-Tucker (KKT) optimality conditions to this problem and devise the so-called "directional water-filling" scheme (DWF) to solve the problem. The word "directional" means the energy flow is right permeable only, which coincides with the causal nature of energy liquidity. Due to the right permeable property, the water level is not equalized in each block, but solely decided by the amount of available energy at that block. Additionally, the authors show that the DWF algorithm is applicable both for maximizing the throughput problem and for minimizing the transmission time problem in a fading channel.

The DWF method is also considered as one of the sub-optimal solutions for the channel training optimization problem in an EH communication system in [25]. The author consider a point-to-point system where the transmitter can only use the energy it harvests. They also assume that the communication within one transmission block is divided into two stages: the training stage and data transmission stage. These two stages present two problems regarding how to optimize the training power and how to optimize the training period. The two problems are solved by adopting two sub-optimal methods: the DWF approximation and rate approximation. The DWF method requires a detailed energy profile in each transmission block while the rate approximation scheme only requires information about the average EH rate, and thus, the second one becomes more attractive.

[26] studies the structural properties of the optimal power allocation in a point-to-point, flat-fading, single-antenna EH system where only the transmitter is powered up by an energy harvester. The authors aim to obtain the maximum throughput of the network and assume that the system operates on two types of side information (SI): causal SI (which contains the past and present channel conditions and harvested energy information) and full SI (which contains the past, present, and future channel conditions and harvested energy information). With the help of dynamic programming and convex optimization techniques, the authors obtain the structural results for the optimal power allocation in both cases. The authors also propose two heuristic schemes to transmit data and evaluate the performance of these two schemes by

numerical simulations.

2.2.2 Two-Hop Systems

In [27], the aforementioned DWF power allocation algorithm is examined in a two-hop communication system with one EH source assisted by a half-duplex non-EH relay node. The authors consider a decode-and-forward relaying scheme with an off-line setting. Two problems, namely short-term throughput maximization problem and transmission completion time minimization problem, are studied. The problems are solved by the DWF algorithm. It is shown that the result obtained by the DWF in the single-hop EH systems provides a guideline for solving the problem in two-hop EH communication systems.

2.3 Systems with Two Energy Harvesting Nodes

For the problems in two EH node systems, it is assumed that both EH nodes have their independent and uncorrelated harvested energy supplies. Additionally, the causality and battery capacity constraints of the two EH nodes have to be jointly considered in the optimization problem.

2.3.1 Multiple-User Interference Channel

[28, 29] consider a two EH transmitter and two receiver system where the EH nodes have finite capacity batteries. The authors provide variant algorithms to maximize the sum-capacity in the interference channels. It is shown that the maximum sum-capacity of the channel can be achieved by solving the optimization problem of the power policy in each EH transmitter. By employing a modified water-filling algorithm in the optimization problem for each transmitter node, the result converges to the optimum.

In [30], the authors aim to achieve the maximum utility in a general wireless network where all the network nodes are EH nodes. In their work, the utility of the network is expressed as a function of the instantaneous power of all EH nodes. Under this assumption, the general utility optimization problem can be solved by achieving the maximum power policy in each node. The authors decompose the optimization problem of each node into a pair of nested problems: an inner problem, which addresses energy efficiency, and an outer problem, which addresses energy allocation for energy harvesting nodes. The decoupled sub-problems are proved to be solved by the generalized DWF algorithm.

2.3.2 Two-Hop Systems

In [31, 32, 33, 34], the authors consider a two-hop system where the transmitter and the relay are EH nodes with infinite battery capacity. In [31], the optimal off-line policy for maximizing the total throughput is developed by observing the properties of the optimal scheme in a half-duplex communication system. Moreover, [32] provides the optimal transmission schemes of the throughput maximization problems, in both half-duplex and full-duplex relaying systems. In this work, the authors introduce an algorithm, namely “max-bit”, to solve the problem in the full-duplex case. Furthermore, the bisection method is carried out to solve a simplified half-duplex relaying model which has only one energy packet at the EH node.

Instead of deriving the optimal policy based on the properties of the optimal transmission, the authors in [35, 36] search for the optimal solution of the throughput maximization problem by applying standard optimization methods. They consider a two-hop AF relay network with an EH transmitter and an EH relay. Specifically, the batteries have finite-capacity, which is consistent with the practical situation. It is shown in [35] that an off-line optimization problem in such a system is a convex mixed integer non-linear program (MINLP) and can be solved by the Generalized Bender’s Decomposition (GDB) method. The idea of the GDB is based on decomposing the problem into a primal problem and a master problem. These two sub-problems will be iteratively solved until the solution converges. This work also proposes two sub-optimal on-line power allocation schemes with relatively low computational complexity. However, the authors in [36] consider a same system and propose an effective Alternate Convex Search algorithm to maximize the total throughput under an off-line setting. Moreover, they also consider an on-line setting in such a system. To overcome the complex computation in the on-line case, they cast the optimization problem as a Markov decision process (MDP). From the discrete point of view, the structural properties of the optimal solution are derived and an MDP-based algorithm is also presented to obtain the optimal policy.

[37] studies a throughput maximization problem in a classic three-node Gaussian relay channel with DF relaying scheme. The transmitter and the relay nodes are assumed to be powered up by the energy drawn from EH devices. The authors consider two types of traffic: delay-constrained (DC) traffic and no-delay-constrained (NDC) traffic. For the DC case, the receiver has to decode the received messages immediately as soon as the messages arrive. For the NDC case, the messages are allowed to be stored for a certain delay before decoding them. Two different algorithms are derived to solve the DC and NDC cases. Finally, the simulation results show that the NDC strictly outperforms the DC since a new form of diversity, namely "energy diversity", can be exploited in the NDC case to increase the throughput. The so-called energy diversity arises from the differences of energy arrivals in time domain.

2.4 Systems with Three Energy Harvesting Nodes

Considering a system with three EH nodes is a relatively new direction in contrast with the aforementioned two models.

Focusing on an off-line throughput maximization problem, [13, 14] consider an MABC-based Gaussian two-way relay channel with two EH transceiver nodes and a half-duplex EH DF relay node. Based on the concavity of the problem, [13] proposes a steepest descent method to solve the concave optimization problem in such a model. The steepest descent algorithm guarantees that the outcome converges to the optimum solution, which yields the maximum sum-throughput. In addition, [14] studies the same problem in both MABC and TDBC protocols. Instead of applying the steepest descent algorithm, [14] solves such a concave problem by using standard convex solver software packages, i.e., CVX in the Matlab tool box.

In [15], the authors aim to maximize the total throughput in the two-way relay EH systems under the assumptions of full-duplex and half-duplex channels. In their systems, both transceivers and the relay are EH nodes and are subject to independent energy causality and battery constraints. The generalized iterative water-filling algorithm is shown to solve the sum-throughput maximization problem under AF, DF, CF, and compute-and-forward schemes. Through computer simulations, the authors find that the DF scheme outperforms other schemes, when at least one node has low transmitting power, while the compute-and-forward scheme performs better when all the nodes have high transmitting power. Based on this observation, the authors continue to propose a novel hybrid scheme, which combines the advantages of two schemes and yields a better performance. Based on the result in [15], the authors in [16] study a problem of how the relay strategies influence the total throughput of the network. An algorithm, which is capable of choosing the proper strategy based on the instantaneous transmitting powers of all nodes, is proposed to improve the throughput. Furthermore, the switching between two relaying strategies can bring an unexpected benefit, namely "time-sharing", to increase the throughput. Hence, this hybrid scheme can outperform the schemes which use a fixed strategy. Focusing on a half-duplex two-way DF relay system with two EH transceivers and one EH relay node, the authors in [38] derive insightful properties of the optimal policy which maximizes the sum-rate of the system by applying KKT conditions. With some mathematical manipulations, the sum-rate maximization problem can be solved by an iterative subgradient descent method which yields a subgradient at every iteration.

2.5 Non-Ideal Energy Harvesting Systems

Several studies focus on non-ideal conditions in EH systems, e.g., non-ideal circuit power (in which the harvested energy supplies not only the data transmission, but also the circuit) and battery imperfection (in which the battery suffers from storage leakage, losses, and capacity fading).

[39] studies a point-to-point EH system where the transmitter is an EH node with a non-ideal circuit power consumption; i.e., the harvested energy is not only for the transmission purpose, but also constantly supplies the circuit, and this is considered non-ideal in an EH system. In this case, there is a trade-off between maximizing energy efficiency (EE) (i.e., maximizing the bits-per-Joule) and maximizing spectrum efficiency (SE) (i.e., maximizing the bits-per-second-per-Hz (bps/Hz)). This problem is non-convex due to the non-ideal property. The authors first consider an off-line setting and put forward an algorithm, which consists of two stages: EE maximizing and SE maximizing, to solve the problem. This algorithm is used along with the nested optimization method in a multiple parallel AWGN channel. An on-line solution, based on the off-line algorithm, is also derived.

Energy storage imperfection can affect the performance of a point-to-point system with an EH transmitter. [40] considers a scenario in which the battery suffers from a battery leakage, and hence, the battery level varies over time. Assuming that the battery leakage rate is constant, the authors first employ a method suggested in [24] to search an optimal scheme for maximizing the total amount of transmitting bits within a given deadline. However, this approach is only available in an off-line setting with a constant leakage rate.

In [41, 42, 43], the authors consider another battery leakage scenario in a complicated EH system. In their system, an EH transmitter is capable of drawing the energy from either the EH device or from its battery. Specifically, energy harvested by the EH device can be imperfectly stored in the battery. To be more accurate, a portion of harvested energy is lost when it is stored in the battery. Therefore, there is a trade-off between using the energy directly from the EH device or storing the harvested energy in the battery. Optimal off-line transmission policies are determined for different cases, i.e., static and fading channels, single-user and broadcast channels, or limited and unlimited battery size. A novel double-threshold policy is proposed to solve all the problems in an off-line setting under different assumptions. The authors then apply dynamic programming to obtain the optimal transmit power schedule in on-line setting.

2.6 Contributions and Summaries

In this thesis, we study an AF two-way relay half-duplex system with EH node(s). We aim to maximize the total throughput in such a wireless communication system over a finite horizon of time slots under energy causality and battery constraints. Two system models are considered in our work: a model with an EH relay node; and a model with two EH transceiver nodes and one EH relay node. We propose off-line algorithms in both cases.

For the one EH node case, most of the studies focus on a point-to-point system [20, 21, 22]. However, we consider a two-way relay model and prove that the total throughput is a concave function with respect to the relay transmitting power. Aiming to maximize the total throughput, we derive several structural properties of the optimal policy based on the concavity of the objective function. From our observation, a method called "breaking-rope" [20, 24] is employed to solve the problem. We then develop a new algorithm to implement the breaking-rope method and prove its optimality.

In the three EH node case, the total throughput is a function of the three parameters which are the transmitting power of three EH nodes. However, in our two-way relay model, this function is not jointly concave in the three parameters, which is different from the problems studied by the previous researchers and challenges us to find a feasible solution. Hence, we have to simplify the objective function to overcome the difficulty in solving the original problem. By relaxing the problem, we aim to find the upper bound of the total throughput. It is shown that the revised function is concave in one parameter when other two parameters are fixed. Thus, the optimal solution can be obtained by using the iterative Alternate Convex Search method. The result of the proposed method addresses the upper bound of the optimal policy. Through computer simulation, we show that our solution performs closely to the best-case and outperforms the breaking-rope method.

Chapter 3

One Energy Harvesting Node Case

3.1 System Model

In this chapter, we consider an AF two-way relay network consisting of two users, denoted as Node 1 and Node 2, and one relay, Node 3, as shown in Figure 3.1. We assume that there is no direct link between the two users, and thus, the two users communicate with each other only through the relay. Since Nodes 1 and 2 are supplied by conventional batteries, their powers are fixed during the transmission. However, the relay is an EH node that can only harvest energy from the surrounding environment and store the energy in its battery for future use. We further assume that all channels are static and that the noises of this network are AWGN. The channel state information (CSI) can be obtained by casual CSI feedback similar to [23]. The constant channel coefficients h_1 and h_2 represent the channel from Node 1 to the relay and from Node 2 to the relay, respectively.

The energy stored in the relay's battery is E_{max} at most and is used only for the purpose of transmission; i.e., the energy for processing will not be taken into account. Moreover, any amount of harvested energy that exceeds the battery capacity E_{max} will be truncated, hence wasted. In our case we will assume an off-line setting. This

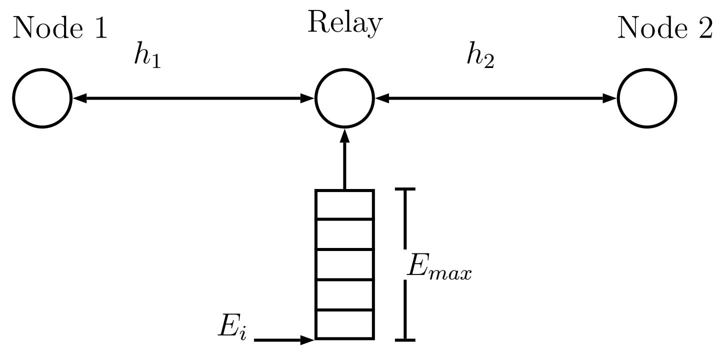

Figure 3.1: A two-way single-relay network with one EH relay node.

meaning that we know exactly how many energy packets will arrive before transmission as well as all arrival instants and the energy amount of each packet. Although this setting is not realistic for an EH system, it can provide a benchmark of the best-case for comparison purpose. The arrival instant vector denoted by $\mathbf{t}$ and the arrival energy vector denoted by $\mathbf{e}$ are expressed, respectively, as $\mathbf{t} = [t_0, t_1, \cdots, t_{N-1}]$ and $\mathbf{e} = [E_0, E_1, \cdots, E_{N-1}]$ with the assumption that there are N energy packets in total. Specifically, the first unit of energy E_0 arrives at t_0, the second energy package E_1 arrives at t_1 and so on.

For the relay, we assume that the energy transmission rate can be changed adaptively during the transmitting process. The power changing action is denoted by an action vector $\mathbf{p}$ with M elements, i.e., $\mathbf{p} \triangleq [p(0), p(1), \cdots, p(M-1)]$, and the corresponding time of each action lasting is recorded in a time duration vector $\mathbf{l}$, where $\mathbf{l} \triangleq [L_0, L_1, \cdots, L_{M-1}]$. We divide the whole transmission process into M transmission blocks according to the number of elements in $\mathbf{p}$, and thus, L_k is the duration for each block with $k = 0, 1, \cdots, M-1$. Specifically, $p(k)$ is the energy transmission rate of the relay employed in the kth block for a period of time L_k. Figure 3.2 illustrates an example schedule that N energy packets arrive in a transmission process which consists of M transmission blocks.

We focus our study on a MABC-based relaying protocol. In Step 1, both users send messages to the relay, and in Step 2, the relay retransmits an amplified version of its received signal. At the first time slot, the signal received at the relay is written

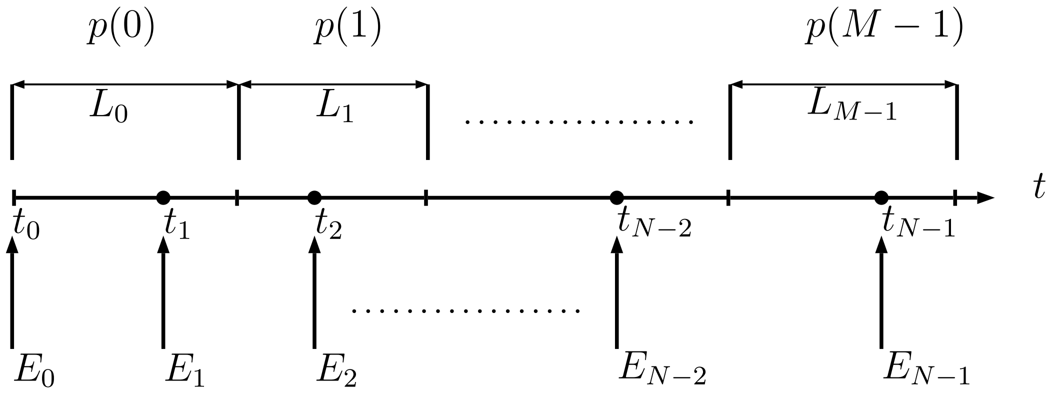

Figure 3.2: Energy harvesting time epoch model in one EH node.

as

$$y_r(q) = \sqrt{p_1}h_1 s_1(q) + \sqrt{p_2}h_2 s_2(q) + n_r(q) \tag{3.1}$$

where p_1 and p_2 are the constant transmitting powers of Nodes 1 and 2, respectively, and $n_r(q)$ is the AWGN receiver noise with variance σ^2 at the relay. We assume that $s_1(q)$ and $s_2(q)$ are the symbols resided in epoch L_k, respectively. In addition, $s_1(q)$ and $s_2(q)$ are uncorrelated with each other and normalized as $\mathbb{E}\{|s_1(q)|^2\} = \mathbb{E}\{|s_2(q)|^2\} = 1$, where $\mathbb{E}\{\cdot\}$ stands for the statistical expectation and $|\cdot|$ represents the absolute value of a complex number. Note that h_1 and h_2 are assumed to be known to both transceivers. At the relay, the received signal is multiplied by an amplification coefficient $\alpha(k)$, and the $\alpha(k)$ which is given by

$$\alpha(k) = \sqrt{\frac{p(k)}{p_1|h_1|^2 + p_2|h_2|^2 + \sigma^2}} \tag{3.2}$$

Thus, the relay's transmitting signal $x_r(q)$ is expressed as

$$\begin{aligned} x_r(q) &= \alpha(k)y_r(q) \\ &= \sqrt{\frac{p(k)}{p_1|h_1|^2 + p_2|h_2|^2 + \sigma^2}}(\sqrt{p_1}h_1 s_1(q) + \sqrt{p_2}h_2 s_2(q) + n_r(q)) \end{aligned} \tag{3.3}$$

In the second time slot, the relay broadcasts the signal $x_r(q)$ to two users. After self-interference-cancellation, the received signals at Nodes 1 and 2, denoted by $y_1(q)$ and $y_2(q)$, respectively, can be written as

$$y_1(q) = \sqrt{p_2} h_1 h_2 \alpha(k) s_2(q) + h_1 \alpha(k) n_r(q) + n_1(q) \tag{3.4}$$

$$y_2(q) = \sqrt{p_1} h_1 h_2 \alpha(k) s_1(q) + h_2 \alpha(k) n_r(q) + n_2(q) \tag{3.5}$$

Assume that the noises $n_1(q)$, $n_2(q)$ and $n_r(q)$ are uncorrelated and i.i.d. Gaussian random variables with zero-mean and variance σ^2. Hence, given (3.2), the received SNRs of the two users is written as

$$\mathrm{SNR}_1(k) = \frac{p_2 p(k) |h_1 h_2|^2 / \sigma^2}{\sigma^2 + p(k)|h_1|^2 + p_1 |h_1|^2 + p_2 |h_2|^2} \tag{3.6}$$

$$\mathrm{SNR}_2(k) = \frac{p_1 p(k) |h_1 h_2|^2 / \sigma^2}{\sigma^2 + p(k)|h_2|^2 + p_1 |h_1|^2 + p_2 |h_2|^2} \tag{3.7}$$

This concludes the system model.

3.2 Problem Formulation

In this section, we aim to maximize the throughput B of the whole system for a certain period of time T which has been divided into M transmission blocks. Essentially, this is a throughput maximization problem; given a finite transmission time T, we aim to transmit as many data bits as possible.

From information theory, in the AWGN channel, the data rates of Nodes 1 and 2 in the kth epoch, denoted by $g_1(p(k))$ and $g_2(p(k))$, respectively, relate to the received

SNRs as described below [22]:

$$
\begin{aligned}
g_1(p(k)) =& \frac{1}{2}\log\Big(1+\mathrm{SNR}_1(k)\Big) \\
=& \frac{1}{2}\log\Big(1+\frac{p_2 p(k)|h_1h_2|^2/\sigma^2}{\sigma^2+p(k)|h_1|^2+p_1|h_1|^2+p_2|h_2|^2}\Big)
\end{aligned} \tag{3.8}
$$

$$
\begin{aligned}
g_2(p(k)) =& \frac{1}{2}\log\Big(1+\mathrm{SNR}_2(k))\Big) \\
=& \frac{1}{2}\log\Big(1+\frac{p_1 p(k)|h_1h_2|^2/\sigma^2}{\sigma^2+p(k)|h_2|^2+p_1|h_1|^2+p_2|h_2|^2}\Big)
\end{aligned} \tag{3.9}
$$

where the factor 1/2 is used to signify that the relay is based on MABC protocol, i.e., one transmission epoch is divided into two equal sections. Thus, the sum-rate of the system $R(\mathbf{p})$ is given by

$$
\begin{aligned}
R(\mathbf{p}) &= \frac{1}{T}\sum_{k=0}^{M-1} L_k g_1\Big(p(k)\Big) + \frac{1}{T}\sum_{k=0}^{M-1} L_k g_2\Big(p(k)\Big) \\
&= \frac{1}{T}\sum_{k=0}^{M-1} \frac{L_k}{2}\log\Big(1+\frac{p_2 p(k)|h_1h_2|^2/\sigma^2}{\sigma^2+p(k)|h_1|^2+p_1|h_1|^2+p_2|h_2|^2}\Big) \\
&+ \frac{1}{T}\sum_{k=0}^{M-1} \frac{L_k}{2}\log\Big(1+\frac{p_1 p(k)|h_1h_2|^2/\sigma^2}{\sigma^2+p(k)|h_2|^2+p_1|h_1|^2+p_2|h_2|^2}\Big)
\end{aligned} \tag{3.10}
$$

Note that $p(k)$ is the relay's transmission policy which we aim to determine and other parameters are known as constants over the whole transmission process in an off-line scheme. Analyzing (3.8) and (3.9), we identify the following properties of $g_1(p(k))$ and $g_2(p(k))$:

- $g_1(0) = 0$ and $g_2(0) = 0$.
- Both $g_1(p(k)) \to \infty$ and $g_2(p(k)) \to \infty$ as $p(k) \to \infty$.
- $g_1(p(k))$ and $g_2(p(k))$ are strictly concave in $p(k)$.

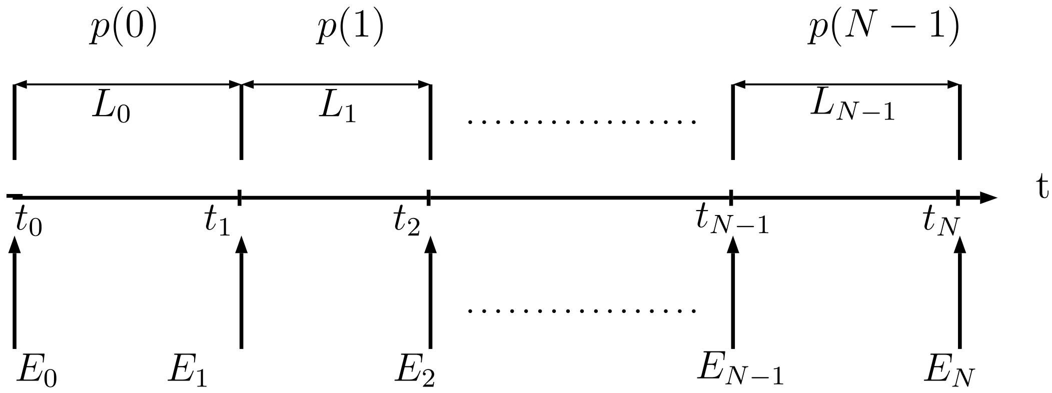

Figure 3.3: Energy harvesting time epoch model in one EH node.

- $g_1(p(k))$ and $g_2(p(k))$ are continuously differentiable.
- $g_1(p(k))/p(k)$ and $g_2(p(k))/p(k)$ decrease monotonically in $p(k)$.

The above properties show that (3.8) and (3.9) satisfy the requirements of the transmission rate function introduced in [44]. As a result, the optimal power transmission rate $p(\cdot)$ can change only when a new energy packet is arrived as shown in Figure 3.3. Hence, M, which is the number of times that the relay can change its power, is equal $N+1$. Note that the relay may not necessarily change its power between two consecutive epochs. For simplicity, we substitute N for M in the following context. In addition, the time span L_k between two adjacent energy arrivals E_k and E_{k+1} can be written as $L_k = t_{k+1} - t_k$, for $k = 0, 1, \cdots, N-1$. Without loss of generality, we assume there is no energy arriving at the last moment $t_N = T$, since $t_N = T$ marks the end of the transmission process, hence we assume that $E_N = 0$ holds true. In conclusion, the optimal energy management policy has a constant energy transmission rate $p(k)$ in the kth epoch for a period of time L_k .

In a practical situation, any energy unit E_k cannot be used ahead of time until it arrives, and thus, an energy causality constraint is considered to restrict the utilization of the harvested energy as

$$\sum_{k=0}^{i} p(k)\frac{L_k}{2} \leq \sum_{k=0}^{i} E_k, \quad \text{for} \quad i = 0, 1 \cdots, N-1 \tag{3.11}$$

where $L_k/2$ indicates the duty ratio of $p(k)$ for the MABC protocol is 1/2.

Limited battery capacity is another constraint which restricts the energy allocation. For example, at any instant t_k, the energy stored in the battery cannot exceed the maximum battery capacity E_{max}. Hence, the following constraint is imposed

$$\sum_{k=0}^{i+1} E_k - \sum_{k=0}^{i} p(k)\frac{L_k}{2} \leq E_{max}, \quad \text{for} \quad i = 0, 1, \cdots, N-1; \tag{3.12}$$

where the left hand side of the inequality indicates the amount of energy left in the battery at the end of the epoch L_k.

Hence, the total number of bits B with the constant energy transmission rate $p(k)$ can be expressed as

$$\begin{aligned} B &= \sum_{k=0}^{N-1} \frac{L_k}{2}\log(1+\mathrm{SNR}_1(p(k))) + \sum_{i=0}^{N-1} \frac{L_k}{2}\log(1+\mathrm{SNR}_2(p(k))) \\ &= \sum_{k=0}^{N-1} \frac{L_k}{2}\log\Big(1+\frac{p_2 p(k)|h_1h_2|^2/\sigma^2}{\sigma^2 + p(k)|h_1|^2 + p_1|h_1|^2 + p_2|h_2|^2}\Big) \\ &+ \sum_{i=0}^{N-1} \frac{L_k}{2}\log\Big(1+\frac{p_1 p(k)|h_1h_2|^2/\sigma^2}{\sigma^2 + p(k)|h_2|^2 + p_1|h_1|^2 + p_2|h_2|^2}\Big) \end{aligned} \tag{3.13}$$

Given that $p(k)$ is an unknown constant in every transmission block, we can optimize $p(k)$ in order to maximize the total number of bits B subject to the constraints in (3.11) and (3.12). The optimization problem can then be written as

$$\text{Q1:} \max_{\mathbf{p}} \quad B$$

$$\text{s.t.} \quad \sum_{k=0}^{i} \frac{L_k}{2} p(k) \leq \sum_{k=0}^{i} E_k, \quad \text{for} \quad i = 0, 1, \cdots, N-1 \tag{3.14}$$

$$\sum_{k=0}^{i+1} E_k - \sum_{k=0}^{i} \frac{L_k}{2} p(k) \leq E_{max}, \quad \text{for} \quad i = 0, 1, \cdots, N-1 \tag{3.15}$$

$$p(k) \geq 0, \quad \text{for} \quad k = 0, 1, \cdots, N-1 \tag{3.16}$$

We maximize the total throughput B by optimizing the energy management policy $\mathbf{p}$ over all blocks. Although this optimization problem can be solved in many ways(one such example is CVX or the `Fmincon` in Matlab), we are going to look at the problem from a different prospective. We aim to characterize the optimal transmission policy and develop a solution which satisfies these characteristics rather than applying standard optimization methods .

3.3 The Optimal Policy

In this section, we search for an efficient method to solve the optimization problem Q1. We start from analyzing the constraints in the problem, then present several lemmas to confine the behavior of the optimal solution. These lemmas are based on certain properties of the objective function and reveal necessary requirements for the optimal power control policy. By observing the behavior of the optimal policy, we finally develop a new algorithm to solve the problem perfectly.

Firstly, we transform (3.15) and rewrite it as

$$\sum_{k=0}^{i} E_k - E_{max} \leq \sum_{k=0}^{i-1} \frac{L_k}{2} p(k), \quad \text{for} \quad i = 1, \cdots, N \tag{3.17}$$

Together with (3.14), the upper bound and lower bound of the consumed energy $\sum_{k=0}^{N-1} L_k p(k)$ can be obtained and given by

$$\sum_{k=0}^{i} E_k - E_{max} \leq \sum_{k=0}^{i-1} \frac{L_k}{2} p(k) \leq \sum_{k=0}^{i-1} E_k, \quad \text{for} \quad i = 1, \cdots, N \tag{3.18}$$

With the knowledge of the arrival instant vector $\mathbf{t}$ and the arrival energy vector $\mathbf{E}$, we depict these two bounds in a stair-step shape as a function of time, and such stair-steps give us a direct graphical visualization. Example 1 in Figure 3.4 offers us some understanding of these constraints. In this example, we assume that 10 energy packets have been harvested and stored in the battery within 5 seconds. The value of each energy unit E_k is a random but known variable, which subjects to the $E_{max} = 15$. Assume that the time period between adjacent packet arrivals is 2 second, i.e., $L_k = 2$ for all k.

By plotting boundaries (3.18) , we show the so-called energy tunnel in Figure 3.4. The space between these two bounds is the range for a feasible energy allocation policy. We call such the area between the two stair-steps as the energy tunnel for the reason that only the energy depletion curve inside this tunnel will correspond to a feasible power policy. Specifically, the height of each block is the maximum battery capacity E_{max}, while the width of each block is the duration of each block.

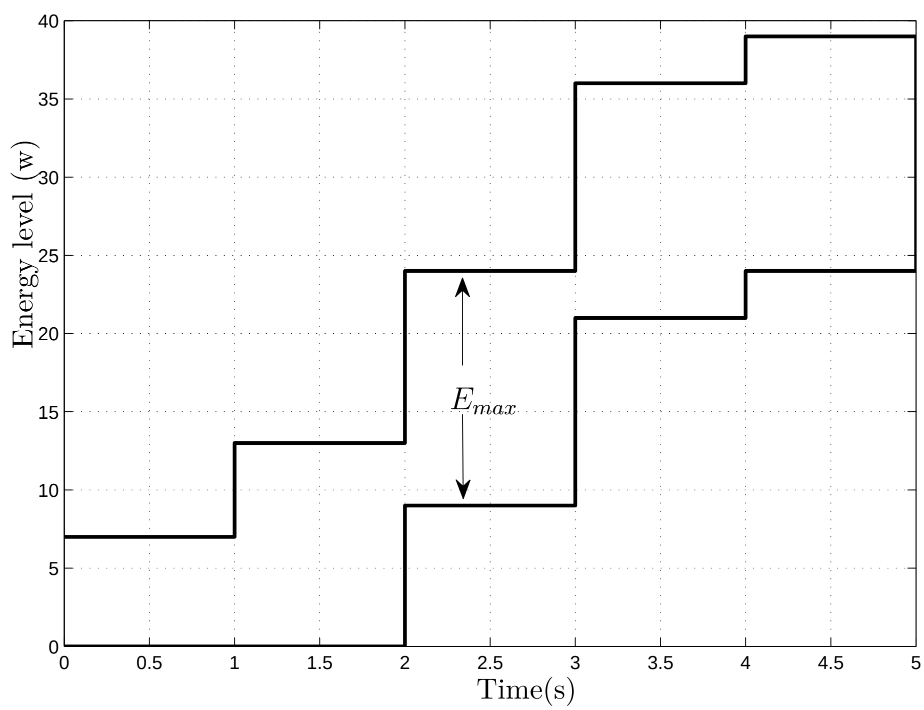

Figure 3.4: Example 1: Energy tunnel.

Inside the tunnel, the energy levels of upper and lower bounds for each block are recorded in two sets, **UB** and **LB**, which are respectively defined as follows:

Definition 1: **UB** *is a set containing the summations of arrival energy at each* *energy arrival instant t_k,*

$$\mathbf{UB} = \Big[E_0, \sum_{k=0}^{1} E_k, \cdots, \sum_{k=0}^{N-1} E_k\Big] \tag{3.19}$$

Definition 2: **LB** *is a set containing the summations of the minimum energy that can be stored in the battery at each energy arrival instant t_k,*

$$\mathbf{LB} = \Big[\max\Big(0, E_0 - E_{max}\Big), \max\Big(0, \sum_{k=0}^{1} E_k - E_{max}\Big), \cdots, \\ \max\Big(0, \sum_{k=0}^{N-1} E_k - E_{max}\Big)\Big] \tag{3.20}$$

From the definition, we know that **UB** is actually the accumulation of harvested energy obtained from the energy causality constraint (3.14). On the other hand, **LB** reflects the battery constraint (3.15). Since **UB** and **LB** indicate the maximum and minimum energy level of each epoch, all curves are considered applicable if they fully fall inside the tunnel. For example, the energy consumption curves 1, 2, 3 and 4 shown in Figure 3.5 are feasible. The ith element in **UB** or **LB** is indexed, respectively, as $UB(i)$ or $LB(i)$. Furthermore, given the energy arrival instant vector $\mathbf{t}$, the coordinates of every sharp corner is known for us, e.g., Point A is at $(t_1, UB(1))$ of the upper bound and Point B is at $(t_2, LB(2))$ of the lower bound in Figure 3.5. Once we have determined the range of all feasible policies, we then need to find the optimal one which is able to maximize the total number of transmitted bits. Derived from the characteristics of the objective function (3.13) in the previous section, the following three lemmas, which are concluded and proven by previous works in a similar problem, describe the behavior of the optimal policy. Readers are referred to [20] and [24] for more details.

Lemma 1: *The energy transmission rate $p(\cdot)$ changes only when the battery is either depleted or full under the optimal power control policy.*

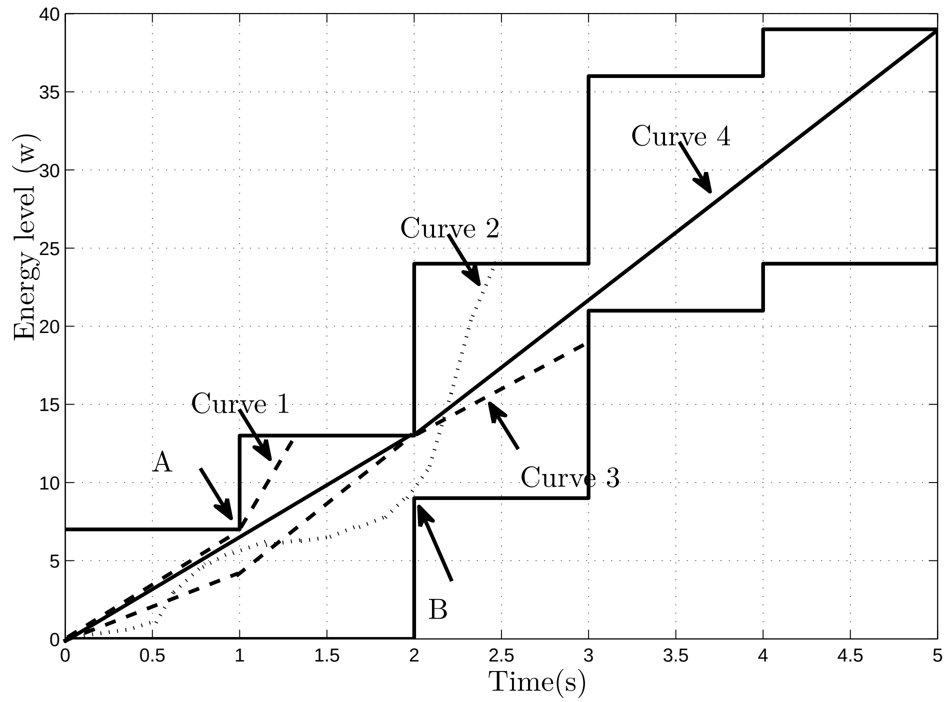

Figure 3.5: Example 1: Feasible depletion curves and sharp corners in the tunnel.

Lemma 2:*For the optimal policy, the energy transmission rate increases if, and only if, the battery is empty; and decreases if, and only if, the battery is full.*

Lemma 3: *For the optimal policy, whenever the transmission ends, the consumed energy will finally be equal to the harvested energy.*

Given the above lemmas, a method, called breaking-rope technique (also known as “string visualization" in some papers) can be used to solve our optimization problem. This method has been widely used in solving similar problems, not only in the energy harvesting field such as [20] and [44], but also in the area of tackling data transmission rate problems in [24]. The breaking-rope suggests that, in such a time-varying energy tunnel, we fix an end of a rope at the starting point of the time line while pulling the rope at the last point of the time line tightly such as Curve 4 in Figure 3.5. The shape of the rope is exactly the optimal energy transmission rate. The general idea of breaking-rope is introduced in Example 2. In this example, we consider the energy tunnel shown in Figure 3.6. In the first step, we link the original point to the last

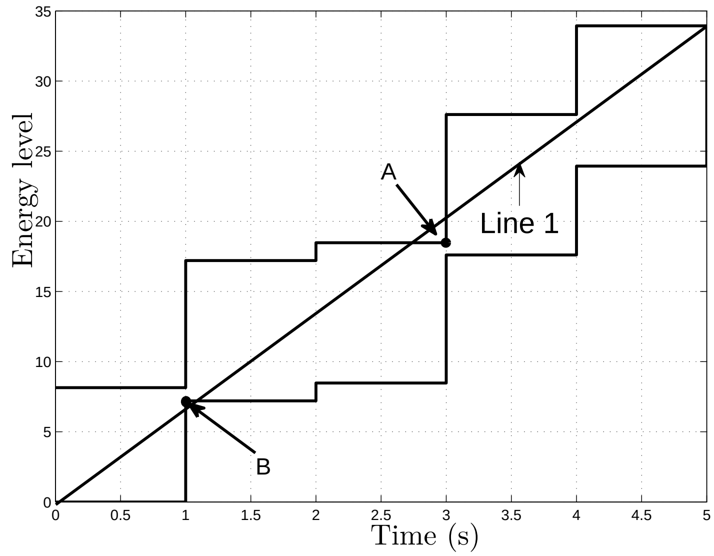

Figure 3.6: Step 1 of Example 2.

point at the tunnel as Line 1. We observe that there are two points which are marked as Point A and Point B laying outside the tunnel at the arrival instants. We than choose the one which is the farthest point away from the tunnel as a breaking point. Point A is the breaking point in this case. In Step 2, we link the original point to the breaking point which is attained from Step 1, and thus, we have Line 2 in Figure 3.7. This time, only one point marked as Point C oversteps the tunnel, and hence, it becomes the new breaking point. We repeat linking the original point to the new breaking point in Step 3 in Figure 3.8. Finally, Line 3 is a segment fully falling inside the tunnel. We assign Line 3 as the first section of the optimal curve, and set the old breaking point C as the new starting point. We repeat Step 1 until another segment, which no part of it falls outside the tunnel, is found. In this way, the optimal energy depletion curve can be obtained segment by segment.

The intuition behind finding the optimal power control policy is based on a goal that tries the best to keep $p(\cdot)$ as a constant. We now study and formulate the behavior of the optimal policy from Lemmas 1, 2 and 3. Based on Lemma 1, we know that the transmission rate $p(\cdot)$ only changes at a certain energy arrival instant

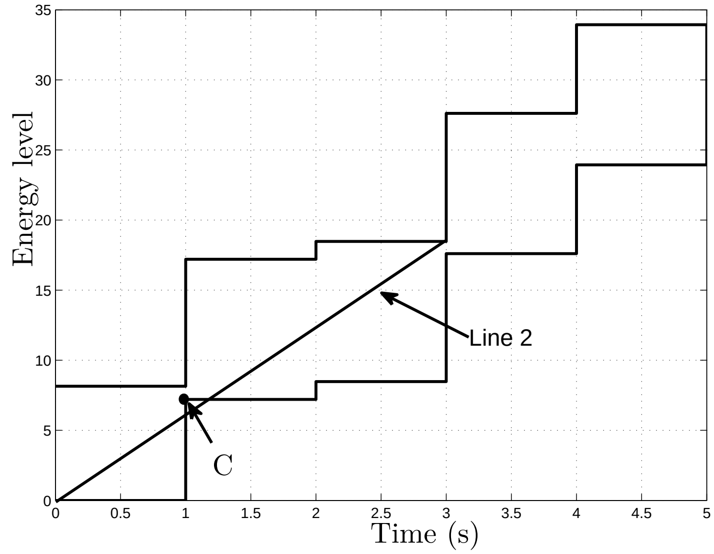

Figure 3.7: Step 2 of Example 2.

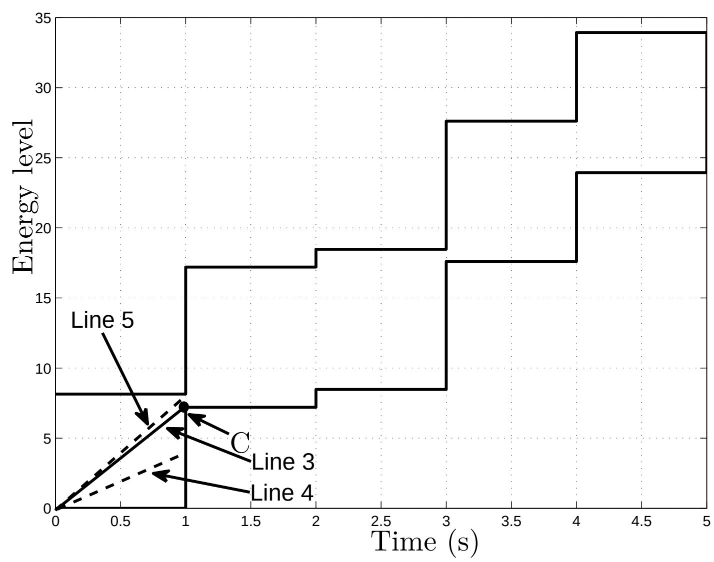

Figure 3.8: Step 3 of Example 2.

t_k which is just the sharp corner inside the tunnel , i.e., point A at the upper bound and point B at the lower bound in Figure 3.6. Lemma 2 tells us at an instant t_k, $p(\cdot)$ can probably increase in the next block if the energy has been depleted; or $p(\cdot)$ may decrease if the energy stored in the battery is full. Lemma 3 implies that the optimal energy depletion curve starts from the origin point and has to end up at the last point of the tunnel. Note that once the depletion curve goes above the tunnel, a battery over-use has happened which violates the energy causality for using a energy packet that has yet to arrive. On the other hand, any part of a curve that falls below the tunnel indicates the case that the energy stored in the battery exceeds the capacity.

For clarity of exposition, we now introduce some parameters that will be used in our algorithm.The starting point $\mathbb{S}$ and ending point $\mathbb{E}$, which contain the coordinates of the two sides of a line, respectively, are defined as below:

$$\mathbb{S} = (\mathbb{S}_x, \mathbb{S}_y) \tag{3.21}$$

$$\mathbb{E} = (\mathbb{E}_x, \mathbb{E}_y) \tag{3.22}$$

where the x-coordinate and y-coordinate are given as

$$\mathbb{S}_x = t_s, \quad \mathbb{S}_y = UB(s+1) \text{ or } LB(s+1) \tag{3.23}$$

$$\mathbb{E}_x = t_e, \quad \mathbb{E}_y = UB(e) \text{ or } LB(e) \tag{3.24}$$

where the starting index s and the ending index e are the subscripts using in $\mathbb{S}$ and $\mathbb{E}$, respectively.

Following the idea of keeping $p(\cdot)$ unchanged as much as possible, we go back to Example 2 again for illustration. First, we set the starting index $s = 0$, and the corresponding starting point $\mathbb{S}$ should be the origin point with $\mathbb{S} = (t_0, LB(1))$. We then set the ending index $e = 5$ and the ending point $\mathbb{E} = (t_5, UB(5))$ under the fact that there are 5 transmission blocks in this case. Linking $\mathbb{S}$ $(t_0, LB(1))$ to $\mathbb{E}$ $(t_5, UB(5))$ as what we done in Step 1 Figure 3.6, Line 1 is obtained. The values of Line 1 at each energy arrival instant t_k are recorded in a vector $\overline{\mathbf{d}}$ which $\overline{\mathbf{d}}$ varies for every iteration. Assume that $\overline{d(k)}$ is an element in $\overline{\mathbf{d}}$, which accordingly represents the value of Line 1 at instant t_k, e.g., $\overline{d(4)}$ is the value of Line 1 at t_4. Obtaining the information of every point in Line 1 for a certain t_k is possible since we have the coordinates of both points $\mathbb{S}$ and $\mathbb{E}$ as well as the time vector $\mathbf{t}$. As we already know that Line 1 has two points A and B, which the coordinate is $(t_3, UB(3))$ and $(t_1, LB(2))$, respectively, locating out of the tunnel. However, we need to find out these two violation points in a mathematical way rather than observing from the figure. Such a procedure is briefly introduced in the following context:

$$\begin{aligned} m &= \min_{s+1 \le k \le e} \{0, UB(k) - \overline{d(k)}\} \\ n &= \min_{s+1 \le k \le e} \{0, \overline{d(k)} - LB(k+1)\} \\ l &= \min\{0, m, n\} \end{aligned} \tag{3.25}$$

If $l = m$, means that the farthest point is located at the upper bound, then we reset the ending point $\mathbb{E}$ and the ending index e as

$$e = \arg \min_{s+1 \le k \le e} \{UB(k) - \overline{d(k)}\} \tag{3.26}$$

$$\mathbb{E} = (t_e, UB(e)) \tag{3.27}$$

If $l = n$, means that the farthest point is located at the lower bound, then we reset

Algorithm 1 The Breaking-rope

Input: N, E_{max}, $\mathbf{t}$ and $\mathbf{E}$.
Output: The optimal transmission rate $\mathbf{p}$.

1: Set $s = 0$, $e = N$.
2: Initialize $\mathbb{S} = (t_0, LB(1))$ and $\mathbb{E} = (t_N, UB(N))$,respectively.
3: **while** $s \neq N$ **do**
4: Obtain $\overline{\mathbf{d}}$ according to $\mathbb{S}$ and $\mathbb{E}$.
5: **if** $\min_{s+1 \leq k \leq e}\{0, UB(k) - \overline{d(k)}, \overline{d(k)} - LB(k+1)\} = 0$
6: **goto** Step 15.
7: **else if** $\min_{s+1 \leq k \leq e}\{UB(k) - \overline{d(k)}\} \leq \min_{s+1 \leq k \leq e}\{\overline{d(k)} - LB(k+1)\}$
8: $e = \arg \min_{s+1 \leq k \leq e}\{UB(k) - \overline{d(k)}\}$ and set $\mathbb{E} = (t_e, UB(e))$
9: **goto** Step 4.
10: **else**
11: $e = \arg \min_{s+1 \leq k \leq e}\{\overline{d(k)} - LB(k)\}$ and set $\mathbb{E} = (t_e, LB(e+1))$.
12: **goto** Step 4.
13: **end if**
14: **end if**
15: $[p(s) : p(e-1)] = \frac{\mathbb{E}_y - \mathbb{S}_y}{\mathbb{E}_x - \mathbb{S}_x}$
16: Set $s = e$ and $\mathbb{S} \leftarrow \mathbb{E}$, set $e = N$ and $\mathbb{E} = (t_N, UB(N))$.
17: **end while**

the ending point $\mathbb{E}$ and the ending index e as

$$e = \arg \min_{s+1 \leq k \leq e}\{\overline{d(k)} - LB(k+1)\} \tag{3.28}$$

$$\mathbb{E} = (t_e, LB(e+1)) \tag{3.29}$$

Specifically, $l = 0$ indicates all the points in $\overline{\mathbf{d}}$ are inside the tunnel, and subsequently, a straight line which linking all the points in $\overline{\mathbf{d}}$ is just the optimal depletion curve without any violation. However, in this example Point A has the farthest distance to the tunnel, and hence is the new breaking point. In Step 2, we set $e = 3$ and update the ending point ($\mathbb{E} \leftarrow$ Point A $(t_3, UB(3))$). Herein the right arrow $\leftarrow$ means assigning the coordinate value of point A to $\mathbb{E}$, e.g., $\mathbb{E} = (t_3, UB(3))$. We repeat linking $\mathbb{S}$ $(t_0, LB(1))$ to $\mathbb{E}$ $(t_3, UB(3))$such as Line 2 in Figure 3.7. By doing so, a new $\overline{\mathbf{d}}$ with information of Line 2 has been obtained. This time, through (3.25), it is shown that only Point C $(t_1, LB(2))$ violates the tunnel. We go on letting ($\mathbb{E} \leftarrow$ Point C

$(t_1, LB(2)))$ and linking $\mathbb{S}$ $(t_0, LB(1))$ to the new $\mathbb{E}$ $(t_1, LB(2))$. Finally, we have Line 3 in Figure 3.8 without any violating point. Thus, the first segment of the optimal policy is obtained. The slope of this segment is the transmission rate $p(\cdot)$ employed during this period of time. We search for the next segment in the same scheme with the updated parameters ($\mathbb{S} \leftarrow$ Point C $(t_1, LB(2)))$ and $(\mathbb{E} = (t_5, UB(5)))$ until the last segment is found. This summarizes the brief idea of our breaking-rope algorithm. Detailed steps are presented in Algorithm 1.

Although the optimization problem Q1 can be solved by any convex optimization problem solver, such as CVX and `Fmincon`, our algorithm still has its own merit. For those classic convex optimization problem solvers, the operating speed is closely related to the amount of data as well as the complexity of the objective function. Furthermore, the computational efficiencies vary from one solver to another since the implement of each solver is different. As for the breaking-rope method, we can obtain the optimal policy only from the energy profiles (which are represented as the constraints) instead of solving the objective function mathematically. In other words, we can get rid of the objective function and find the optimal power allocation only relying on the constraints. Hence, our algorithm is easy in implementation because the operating speed is solely related to the amount of data.

Theorem 1: *Algorithm 1 yields the optimal solution for the maximization problem* (3.13)*.*

Proof: We prove the optimality of Algorithm 1 by analyzing the procedure mentioned in (3.25). The while loop in Algorithm 1 is actually the repeat of the procedure (3.25). For one iteration, we fix the starting point $\mathbb{S}$ and keep updating the ending point $\mathbb{E}$ through (3.25) until the l in (3.25) is equal to 0. However, the final ending point $\mathbb{E}$ is located either in the upper bound or the lower bound.

First, we assume the lower bound case which is the example depicted in Figure 3.8 where Line 3 is the global optimal curve obtained by Algorithm 1 within the epoch $[0, 1]$. Curves that locate below Line 3, such as the dashed Line 4, are obviously sub-

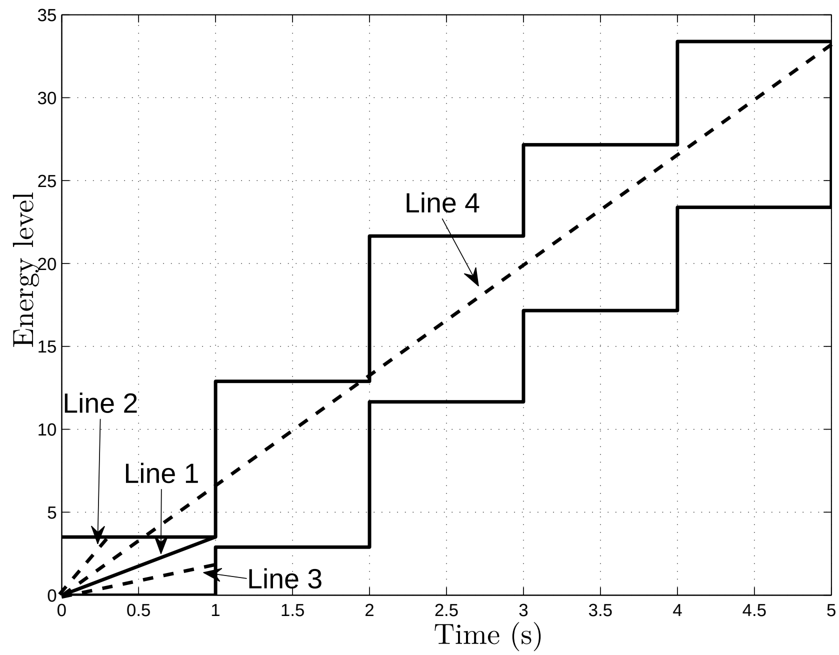

Figure 3.9: An example of Algorithm 1.

optimal since they cause battery overflow. The curves falling above Line 3, such as dashed Line 5, can transmit much more data than our solution within the duration $[0,1]$. However, from Figures 3.6 and 3.7 we know that, if a curve cannot encounter point C in Figure 3.8, it will not encounter any point in the lower bound, and hence will have to keep an non-decreasing slope until the end of the transmission according to lemma 2. The consequence of such policies will definitely cause a battery depletion before the end of the transmission, which violates the optimal property. Therefore, Line 3 is the global optimal curve in the duration $[0,1]$.

We next prove the case that the ending point is in the upper bound. As shown in Figure 3.9, Line 1 is the optimal curve we obtained from Algorithm 1. Any curve that falls below Line 1, such as the dashed Line 3, obviously transmits less data than Line 3 within the duration $[0,1]$. On the other hand, the curve that falls above Line 1, such as dashed Line 2, can cause the battery depletion during this epoch. Thus, this policy cannot keep a constant rate during this epoch and is suboptimal. From the dashed Line 4 we know that the slope of next segment of Line 1 is increasing, and this tendency satisfies lemma 2 and is feasible. Thus, the optimality of one segment which is yielded by Algorithm 1 has been proven. In this way, the optimality of the completed policy throughout the transmission can be proven segment by segment. □

3.4 Numerical Results

In this section, simulation results are presented to illustrate the performance of the breaking-rope in obtaining the optimal policy . Throughout the simulations, the noise power σ^2 is equal to 1 and the harvested energy E_k is assumed to be uniformly distributed in the interval $[0, E_{max}]$. We consider a static channel and hence $h_1 = h_2 = 1$.

Figures 3.10 and 3.11 show the energy depletion curve in the energy tunnel for the breaking-rope method, `fmincon` solver and CVX solver. The length L_k of each block is equal 2 in Figure 3.10 while it is uniformly distributed which takes the values between $[0, 4]$ in Figure 3.11. The energy supply for user nodes p_1 and p_2 are all equal to 10 power units. The relay battery capacity E_{max} is 10 energy units and the harvested energy E_k is taken within $[0, 10]$ with uniform distribution. As can be seen from these figures, the breaking-rope, as well as `fmincon` and CVX, all obtain the same depletion curve.

In Figure 3.12, the total throughput curve of the system is presented versus the number of transmission intervals with $E_{max} = 10$. The number of transmission blocks N is chosen $[10 : 1 : 30]$. In this case, we apply the breaking-rope method to solve the problem and obtain the optimal energy transmission rate $\mathbf{p}$. The throughput can be computed by plugging $\mathbf{p}$ back to the objective function (3.13). This figure is well understanding: the increasing of the throughput is attributed to the number of transmission blocks. Since the more blocks we have, the more energy packets can arrival and the more energy can be applied.

Figure 3.13 depicts total transmission data versus maximum arrival energy. As

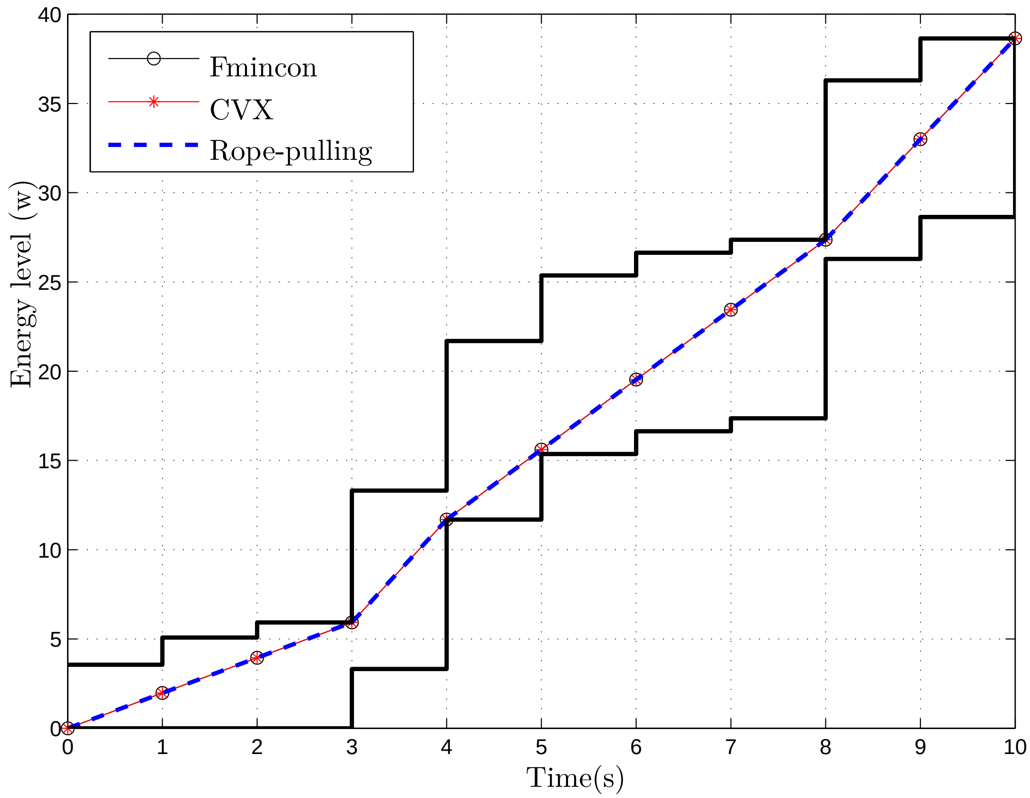

Figure 3.10: Fixed length of transmission block with $L_k = 2$.

mentioned above, the arrival energy E_k of each block takes the value from $[0, E_{max}]$ with uniform distribution. E_{max} is equal to $[1 : 1 : 10]$ in this case with a certain number of transmission blocks $N = 10$. A larger E_{max} not only implies a higher probability of harvesting more energy in each transmission block, but also means more power can be stored in the battery. As a result, t he total throughput is definitely increasing if the system can supply much more energy to the wireless network.

3.5 Summary

In this chapter, we studied the problem of maximizing the total number of bits of a two-way relay energy harvesting system in an off-line setting. Such maximizing

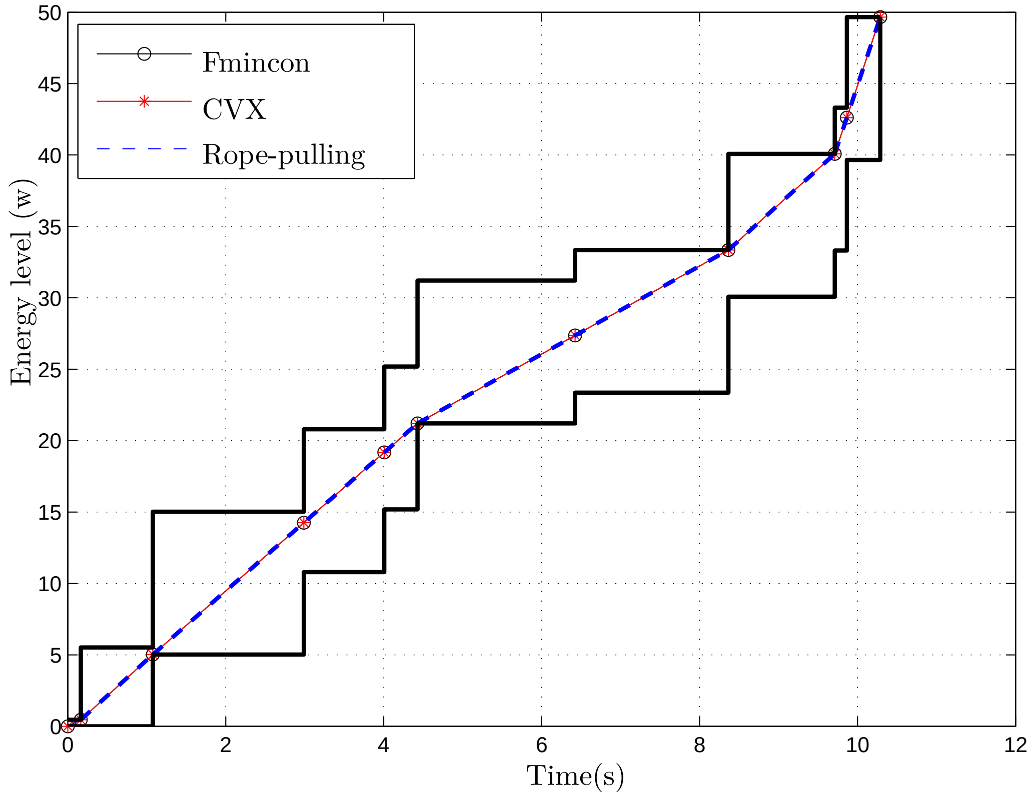

Figure 3.11: Various length of transmission block with random L_k.

problem was solved by optimizing the energy control policy $\mathbf{p}$ in the relay. First, we showed that the objective function in our optimization problem is concave. Then, we showed several properties for the optimal energy allocation policy based on characteristics of the objective function and derived a method to solve the problem. At last, the outcomes of the proposed method was compared with other solvers such as CVX and `Fmincon` in the simulation section. The results shown that the proposed method yields the optimal policy as same as CVX and `Fmincon`. In addition, the properties of the optimal solution was shown in the figure through computer simulations.

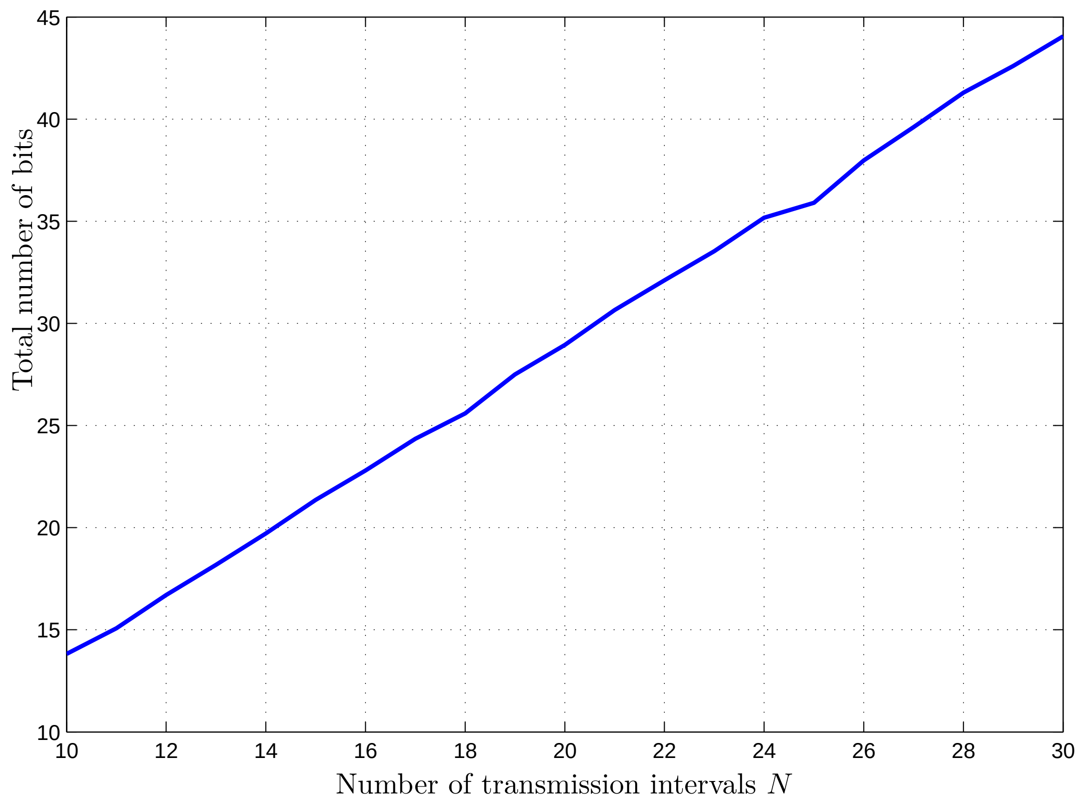

Figure 3.12: Total transmission data versus number of transmission intervals.

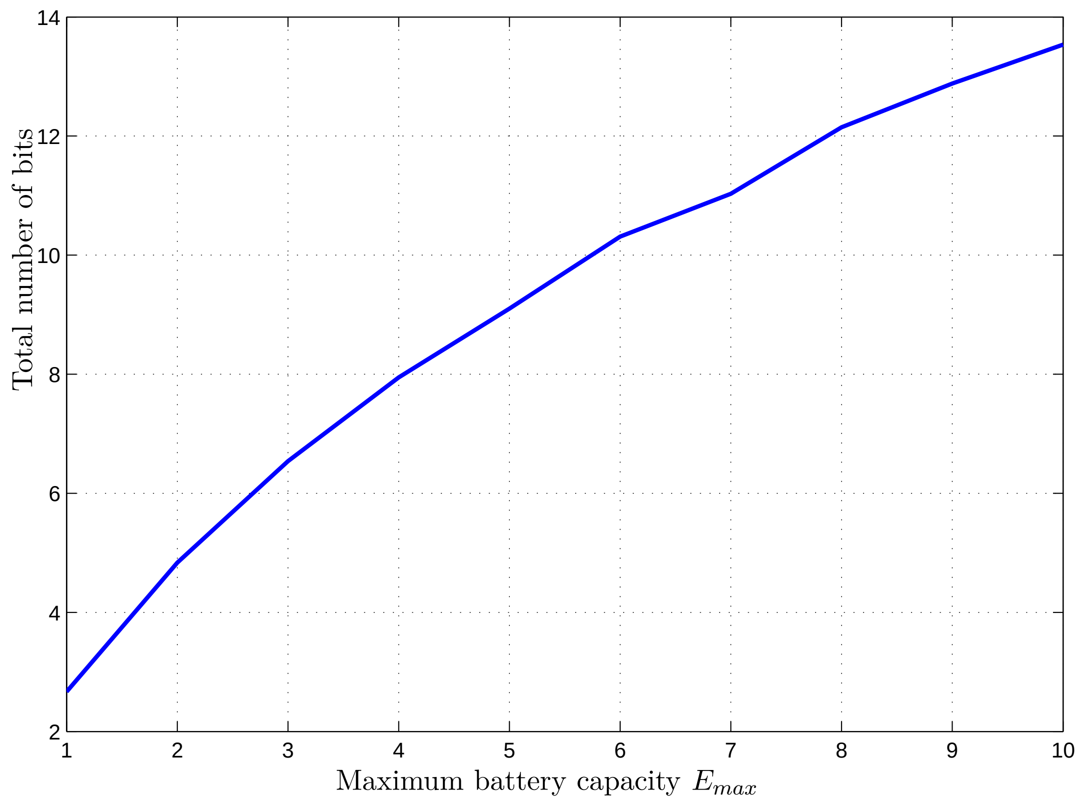

Figure 3.13: Total transmission data versus maximum arrival energy.

Chapter 4

Three Energy Harvesting Node Case

In the previous section, we considered a wireless network consisting of only one EH node. Then, we introduced an algorithm to maximize the total number of transmitted bits by optimizing the EH node's power allocation. In this section, we consider a similar wireless system with three EH nodes. In this type of frame work, not only the relay, but also the two user nodes are equipped with energy harvesting units. In such a network, we aim to maximize the total throughput of the whole system by optimally determining the source and the relay power control policies.

4.1 System Model and Problem Formulation

Figure 4.1 shows a revised system model where three EH nodes exist. We still consider a MABC-based AF relay protocol as previous chapter. This time, all Nodes 1, 2 and the relay, Node 3, are EH nodes. The jth node has its own maximum battery capacity $E_{max,j}$ for $j = 1, 2, 3$. In addition, the causality constraint and battery

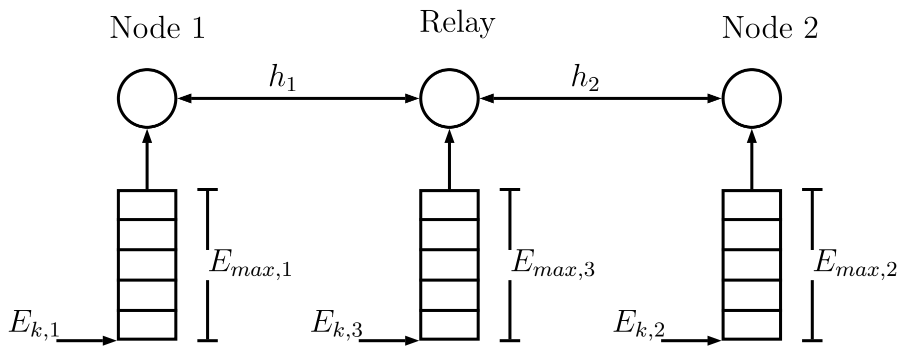

Figure 4.1: A two-way multi-relay network in three EH node.

constraint at the jth node are also independent and uncorrelated with other nodes. Let $E_{k,j}$ denote the energy package arriving in the Node j at instant t_k. Note that the energy packet may not arrive at each arrival instant for all the nodes, i.e., at a certain instant t_k, the energy packet may only arrive in Node 1, and thus, $E_{k,2} = E_{k,3} = 0$. We assume an off-line setting in this system as in previous chapter so that each $E_{k,j}$ and t_k are known to us before the transmission.

We consider a transmission process with N energy packet arrivals during T seconds. The corresponding arrival instant vector $\mathbf{t}$ can be written as $\mathbf{t} \triangleq [t_0, t_1, \cdots, t_N]$. Specifically, there is no energy arrival at the last instant t_N, that is $t_N = T$ only marks the end of the transmission, thus, $E_{N,j} = 0$ for all j. The average transmission power of the jth node allocated in the kth epoch is denoted by $p_j(k)$ so that the transmission policy of the jth node can be written as a vector $\mathbf{p}_j$ with $\mathbf{p}_j \triangleq [p_j(0), p_j(1), \cdots, p_j(N-1)]$ for $j = 1, 2, 3$. For each $p_j(k)$, the epoch duration is denoted as L_k and $L_k = t_{k+1} - t_k$ by definition. Therefore, the total amount of the consumed energy for the jth node in the kth block can be represented by $L_k p_j(k)/2$, where the factor $1/2$ comes from the fact that the relaying scheme is half-duplex. Figure 4.2 illustrates an example time-table of energy packet arrivals and power allocation scheduling in such scenario, where $p_j(k)$, for $j = 1, 2, 3$, may not have to change between two consecutive blocks.

Here, the power management policy is more complicated given three EH nodes exist in the current system. For each node, the energy allocation depends not only

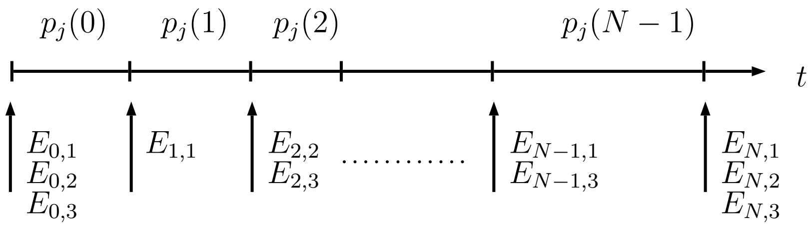

Figure 4.2: Energy harvesting time epoch model.

on the amount of the available energy at that node, but also the amount of energy available at the other two nodes. The total number of transmitting bits B for N transmission blocks is given by

$$B(\mathbf{p_1}, \mathbf{p_2}, \mathbf{p_3}) = \sum_{k=0}^{N-1} \frac{L_k}{2} \log\Big(1 + \frac{p_2(k)p_3(k)|h_1h_2|^2/\sigma^2}{\sigma^2 + p_3(k)|h_1|^2 + p_1(k)|h_1|^2 + p_2(k)|h_2|^2}\Big) + \sum_{k=0}^{N-1} \frac{L_k}{2} \log\Big(1 + \frac{p_1(k)p_3(k)|h_1h_2|^2/\sigma^2}{\sigma^2 + p_3(k)|h_2|^2 + p_1(k)|h_1|^2 + p_2(k)|h_2|^2}\Big) \quad (4.1)$$

Note that (4.1) is not jointly concave in $\mathbf{p}_1$, $\mathbf{p}_2$ and $\mathbf{p}_3$. As a result, maximizing (4.1) by jointly optimizing $\mathbf{p}_1$, $\mathbf{p}_2$ and $\mathbf{p}_3$ may not be amenable to a computationally affordable solution. Specifically, in the right hand side of (4.1), there are two terms hindering us from deciding the concavity of this function, which are $p_1(k)|h_1|^2$ in the denominator of the first term and $p_2(k)|h_2|^2$ in the denominator of the second term. However, we eliminate these two terms in the equation and aim to find the upper bound of B at the best-case scenario. The upper bound of the total throughput is denoted by B_{ub} and is formulated as

$$B_{ub}(\mathbf{p_1}, \mathbf{p_2}, \mathbf{p_3}) = \sum_{k=0}^{N-1} \frac{L_k}{2} \log\Big(1 + \frac{p_2(k)p_3(k)|h_1h_2|^2/\sigma^2}{\sigma^2 + p_3(k)|h_1|^2 + p_2(k)|h_2|^2}\Big) + \sum_{k=0}^{N-1} \frac{L_k}{2} \log\Big(1 + \frac{p_1(k)p_3(k)|h_1h_2|^2/\sigma^2}{\sigma^2 + p_3(k)|h_2|^2 + p_1(k)|h_1|^2}\Big) \quad (4.2)$$

The new equation (4.2) is concave in $\mathbf{p}_1$, $\mathbf{p}_2$, or $\mathbf{p}_3$ when other parameters are fixed.

Thus, we maximize the sum-throughput B_{ub} by jointly optimizing the power allocation $\mathbf{p}_1$, $\mathbf{p}_2$ and $\mathbf{p}_3$. The joint optimization problem can be formulated as

$$
\begin{aligned}
\text{Q2:} \max_{\mathbf{p}_1,\mathbf{p}_2,\mathbf{p}_3} \quad & \sum_{k=0}^{N-1} \frac{L_k}{2}\log\Big(1+\frac{p_2(k)p_3(k)|h_1h_2|^2/\sigma^2}{\sigma^2+p_3(k)|h_1|^2+p_2(k)|h_2|^2}\Big) \\
& + \sum_{k=0}^{N-1} \frac{L_k}{2}\log\Big(1+\frac{p_1(k)p_3(k)|h_1h_2|^2/\sigma^2}{\sigma^2+p_3(k)|h_2|^2+p_1(k)|h_1|^2}\Big) \qquad (4.3)\\
\text{s.t.} \quad & \sum_{k=0}^{i} \frac{L_k}{2}p_j(k) \le \sum_{k=0}^{i} E_{j,k}, \quad \text{for} \quad i=0,\cdots,N-1; \quad j=1,2,3 \qquad (4.4)\\
& \sum_{k=0}^{i+1} E_{j,k} - \sum_{k=0}^{i} \frac{L_k}{2}p_j(i) \le E_{max,j}, \quad \text{for} \quad i=0,\cdots,N-1; \quad j=1,2,3 \\
& \qquad (4.5)\\
& p_j(k) \ge 0, \quad \text{for} \quad k=0,\cdots,N-1; \quad j=1,2,3 \qquad (4.6)
\end{aligned}
$$

The optimization problem Q2 is not jointly concave in $\mathbf{p}_1$, $\mathbf{p}_2$ and $\mathbf{p}_3$. However, we will propose a new method, based biconvexity, to solve this problem in the following section.

4.2 Biconvex Optimization and Alternate Convex Search

In this section, we analyze the characteristic of the objective function in (4.3) and show that it is biconvex with respect to $\mathbf{p}_1$, $\mathbf{p}_2$ and $\mathbf{p}_3$, respectively. Due to the biconvexity property, one iterative approach, which alternatively searches the optimal power allocations for $\mathbf{p}_1$, $\mathbf{p}_2$ and $\mathbf{p}_3$, is proposed to solve the optimization problem

Q2. This approach is introduced in [45] and the biconvexity property is defined as below:

Definition 5: *A function f(x,y):* $X \times Y \rightarrow \mathbb{R}$ *is called a* **biconvex function** *if*

$$f_x(\cdot) = f(x, \cdot) : Y \rightarrow \mathbb{R} \tag{4.7}$$

is a convex function on Y *for every fixed* $x \in X$ *and*

$$f_y(\cdot) = f(y, \cdot) : X \rightarrow \mathbb{R} \tag{4.8}$$

is a convex function on X *for every fixed* $y \in Y$*.*

In our problem, it can be readily proven that (4.3) is concave in $\mathbf{p}_i$ (for $i = 1, 2, 3$) if the other two parameters $\mathbf{p}_j$ (for $j \neq i$) is fixed, i.e., when $\mathbf{p}_2$ and $\mathbf{p}_3$ are fixed, (4.3) is concave in $\mathbf{p}_1$. For any concave problem, it can be turned into a convex problem by simply adding a negative sign. Therefore, Q2 is a biconvex optimization problem and can be solved by an iterative algorithm based on Alternate Convex Search (ACS).

Joint Optimization of $\mathbf{p}_1$, $\mathbf{p}_2$ and $\mathbf{p}_3$

Following the property of biconvexity from last section, we can solve the problem by searching for the optimal value of one parameter while fixing the other two parameters. Hence in the ACS technique, we decompose Q2 into three sub-problems to find the optimal policy for $\mathbf{p}_1$, $\mathbf{p}_2$, and $\mathbf{p}_3$, respectively. The sub-problem Q3 is one of them, which aims to find the optimal $\mathbf{p}_1$ for given $\mathbf{p}_2$ and $\mathbf{p}_3$, and written as below:

$$
\begin{aligned}
\text{Q3} : \max_{\mathbf{p}_1} \quad & \sum_{k=0}^{N-1} \frac{L_k}{2} \log\Big(1 + \frac{p_2(k)p_3(k)|h_1h_2|^2/\sigma^2}{\sigma^2 + p_3(k)|h_1|^2 + p_2(k)|h_2|^2}\Big) \\
& + \sum_{k=0}^{N-1} \frac{L_k}{2} \log\Big(1 + \frac{p_1(k)p_3(k)|h_1h_2|^2/\sigma^2}{\sigma^2 + p_3(k)|h_2|^2 + p_1(k)|h_1|^2}\Big) && (4.9) \\
\text{s.t.} \quad & \sum_{k=0}^{i} \frac{L_k}{2} p_1(k) \le \sum_{k=0}^{i} E_{1,k}, \quad \text{for} \quad i = 0, 1, \cdots, N-1 && (4.10) \\
& \sum_{j=0}^{i+1} E_{1,j} - \sum_{k=0}^{i} \frac{L_k}{2} p_1(k) \le E_{max,1}, \quad \text{for} \quad i = 0, 1, \cdots, N-1 && (4.11) \\
& p_1(k) \ge 0, \quad \text{for} \quad k = 0, \cdots, N-1 && (4.12)
\end{aligned}
$$

where $\mathbf{p}_2$ and $\mathbf{p}_3$ are assumed to be given in this problem. As a result, Q3 is concave with respect to $\mathbf{p}_1$. To tackle this convex sub-problem, any conventional convex solvers such as Matlab's CVX solver can be applied. The solution to Q3 updates the value of $\mathbf{p}_1$. We will use this updated $\mathbf{p}_1$ to search $\mathbf{p}_2$ and $\mathbf{p}_3$ in the follow procedures. In the next step, given $\mathbf{p}_1$ and $\mathbf{p}_3$, we find the optimal policy of $\mathbf{p}_2$ by replacing the unknown parameter $\mathbf{p}_1$ with $\mathbf{p}_2$ in Q3. The second sub-problem Q4 is formulated as

$$
\begin{aligned}
\text{Q4} : \max_{\mathbf{p}_2} \quad & \sum_{k=0}^{N-1} \frac{L_k}{2} \log\Big(1 + \frac{p_2(k)p_3(k)|h_1h_2|^2/\sigma^2}{\sigma^2 + p_3(k)|h_1|^2 + p_2(k)|h_2|^2}\Big) \\
& + \sum_{k=0}^{N-1} \frac{L_k}{2} \log\Big(1 + \frac{p_1(k)p_3(k)|h_1h_2|^2/\sigma^2}{\sigma^2 + p_3(k)|h_2|^2 + p_1(k)|h_1|^2}\Big) && (4.13) \\
\text{s.t.} \quad & \sum_{k=0}^{i} \frac{L_k}{2} p_2(k) \le \sum_{k=0}^{i} E_{2,k}, \quad \text{for} \quad i = 0, 1, \cdots, N-1 && (4.14) \\
& \sum_{j=0}^{i+1} E_{2,j} - \sum_{k=0}^{i} \frac{L_k}{2} p_2(k) \le E_{max,2}, \quad \text{for} \quad i = 0, 1, \cdots, N-1 && (4.15) \\
& p_2(k) \ge 0, \quad \text{for} \quad k = 0, \cdots, N-1 && (4.16)
\end{aligned}
$$

where Q4 is concave in $\mathbf{p_2}$. Note that the value of $\mathbf{p_1}$ above is obtained from previous sub-problem Q3. The result of Q4 will give us a new $\mathbf{p}_2$. Finally, using the new values of $\mathbf{p}_1$ and $\mathbf{p}_2$ determined by solving Q3 and Q4, we can obtain a $\mathbf{p}_3$ by solving the optimization problem Q5 given below:

$$
\begin{aligned}
\text{Q5}: \max_{\mathbf{p}_3} \quad & \sum_{k=0}^{N-1} \frac{L_k}{2} \log\Big(1 + \frac{p_2(k)p_3(k)|h_1h_2|^2/\sigma^2}{\sigma^2 + p_3(k)|h_1|^2 + p_2(k)|h_2|^2}\Big) \\
& + \sum_{k=0}^{N-1} \frac{L_k}{2} \log\Big(1 + \frac{p_1(k)p_3(k)|h_1h_2|^2/\sigma^2}{\sigma^2 + p_3(k)|h_2|^2 + p_1(k)|h_1|^2}\Big) && (4.17) \\
\text{s.t.} \quad & \sum_{k=0}^{i} \frac{L_k}{2} p_3(k) \leq \sum_{k=0}^{i} E_{3,k}, \quad \text{for} \quad i = 0, 1, \cdots, N-1 && (4.18) \\
& \sum_{j=0}^{i+1} E_{3,j} - \sum_{k=0}^{i} \frac{L_k}{2} p_3(k) \leq E_{max,3}, \quad \text{for} \quad i = 0, 1, \cdots, N-1 && (4.19) \\
& p_3(k) \geq 0, \quad \text{for} \quad k = 0, \cdots, N-1 && (4.20)
\end{aligned}
$$

This describes one iteration of the ACS algorithm.

Iterative Procedure for Joint Power Optimization

To start with the ACS algorithm, a stopping criterion ϵ and the initial values $\mathbf{p}_1^{(0)}$, $\mathbf{p}_2^{(0)}$, and $\mathbf{p}_3^{(0)}$ should be chosen. Note that the initial values should be chosen in their feasible sets in order to ensure the feasibility of the solution, i.e., $0 \leq p_j(k) \leq 2E_{j,k}/L_k$ for all j and k. In the lth iteration, three local optimal values $\mathbf{p}_1^{(l+1)}$, $\mathbf{p}_2^{(l+1)}$, and $\mathbf{p}_3^{(l+1)}$ will be obtained, such values are taken as the input values for the next iteration. At the end of each iteration, the total throughput $B_{ub}(\mathbf{p}_1^{(l+1)}, \mathbf{p}_2^{(l+1)}, \mathbf{p}_3^{(l+1)})$ will be compared with the result $B_{ub}(\mathbf{p}_1^{(l)}, \mathbf{p}_2^{(l)}, \mathbf{p}_3^{(l)})$ from the last iteration to decide whether the stopping criterion is satisfied. In this way, the algorithm is conducted to

Algorithm 2 Alternate Convex Search Method

1: **Initialize:** Set feasible $\mathbf{p}_1^{(0)}, \mathbf{p}_2^{(0)}, \mathbf{p}_3^{(0)}$ and a stopping criterion ϵ;
set $l = 0$.
2: **while** (1) **do**
3: Given the known $\mathbf{p}_2^{(l)}$ and $\mathbf{p}_3^{(l)}$, solve the convex optimization problem Q3 in (4.9) for $\mathbf{p_1}$ and the outcome of this step is denoted by $\mathbf{p}_1^{(l+1)}$.
4: Given the known $\mathbf{p}_1^{(l+1)}$ and $\mathbf{p}_3^{(l)}$, solve the convex optimization problem Q4 in (4.13) for $\mathbf{p_2}$ and the outcome of this step is denoted by $\mathbf{p}_2^{(l+1)}$.
5: Given the known $\mathbf{p}_1^{(l+1)}$ and $\mathbf{p}_2^{(l+1)}$, solve the convex optimization problem Q5 in (4.17) for $\mathbf{p_3}$ and the outcome of this step is denoted by $\mathbf{p}_3^{(l+1)}$.
6: Set $l = l + 1$.
7: **If**$(\|B_{ub}(\mathbf{p}_1^{(l)}, \mathbf{p}_2^{(l)}, \mathbf{p}_3^{(l)}) - B_{ub}(\mathbf{p}_1^{(l-1)}, \mathbf{p}_2^{(l-1)}, \mathbf{p}_3^{(l-1)})\| \geq \epsilon)$
8: **goto** Step 10.
9: **end while**
10: **Output:** $\mathbf{p}_1^{(l)}$,$\mathbf{p}_2^{(l)}$ and $\mathbf{p}_3^{(l)}$.

alternatively search for the optimal value of each variable. Detailed steps are described in Algorithm 2. The outputs of Algorithm 2, denoted by $\mathbf{p}_1^{(l)}$,$\mathbf{p}_2^{(l)}$, and $\mathbf{p}_3^{(l)}$, contains the optimal power allocations for the three nodes over all blocks. The final result converges to an optimal solution. However, due to the original objective function Q2 is not a convex optimization problem, the globally optimality may not guaranteed.

4.3 Numerical Results

In this section, we present our simulation results of the ACS method in a three EH nodes system. We also evaluate the performance of the breaking-rope method in such scenario. In our simulation, three EH nodes have the same maximum battery capacity E_{max}, i.e., $E_{max,1} = E_{max,2} = E_{max,3} = E_{max}$. For clarity of exposition, the lengths L_k between every harvesting energy arrival are all equal to 2. The noise power σ^2 is 1 for all cases.

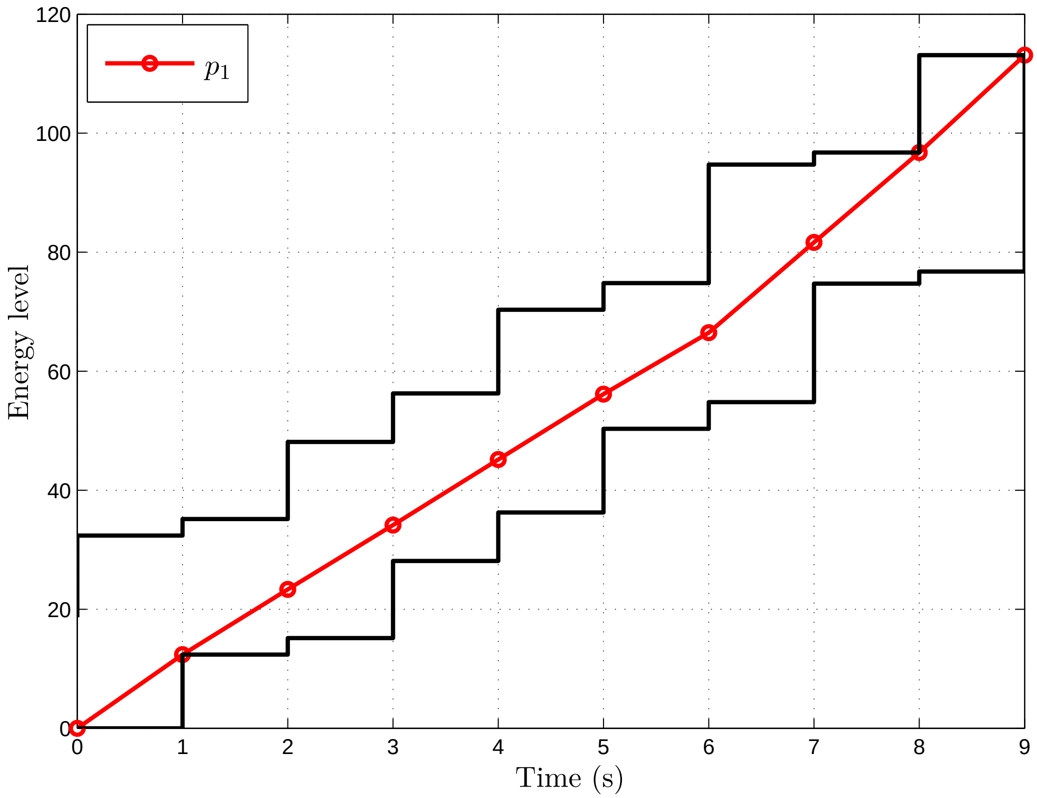

Figure 4.3: Depletion curve of Transceiver 1.

Figures 4.3, 4.4 and 4.5 show the output of Algorithm 2. We use CVX to solve Q3, Q4 and Q5. The optimal depletion curves of $\mathbf{p}_1$, $\mathbf{p}_2$, and $\mathbf{p}_3$ for one realization are depicted in the energy tunnel, respectively. In this case, we choose the maximum battery capacities $E_{max} = 20$ for all three nodes. The total transmission time $T = 9$ is chosen. The channel information h_1 and h_2 are complex values with normally distribution. The tolerance error ϵ for Algorithm 2 is equal to 0.0002. As seen in these figures, the depletion curves may increase at some instants even though they do not hit the sharp corner of the energy tunnel. This observation differs from the optimal property we discussed in the previous chapter since the objective function

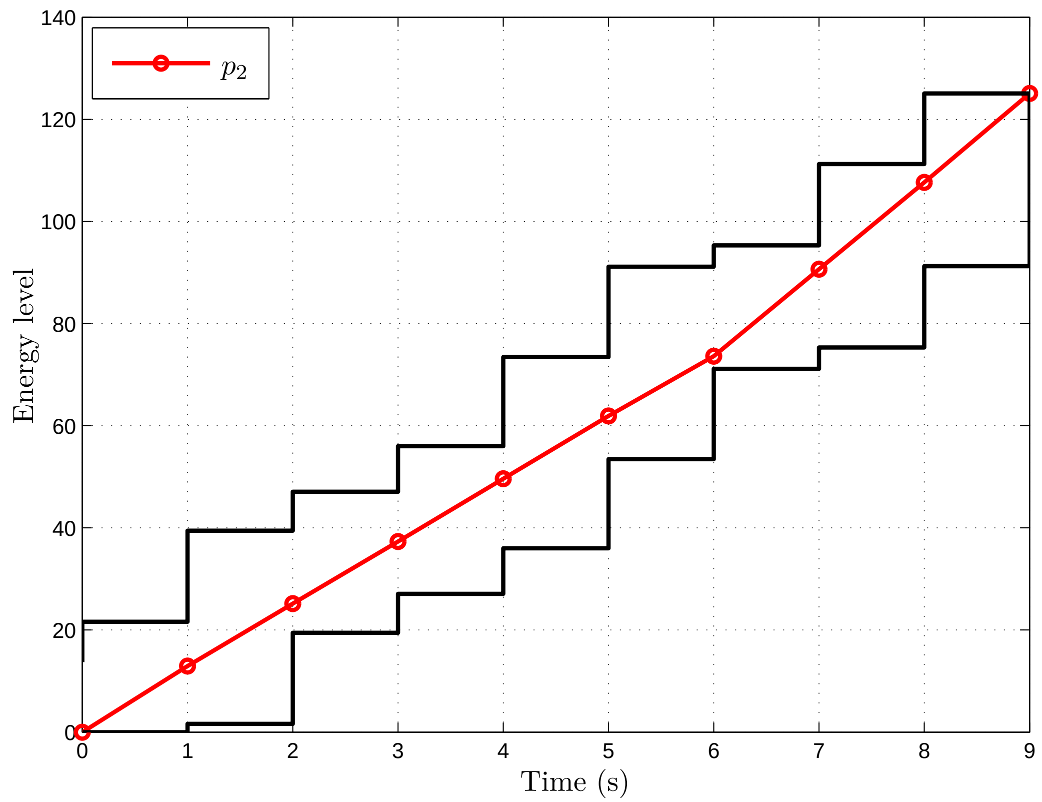

Figure 4.4: Depletion curve of Transceiver 2.

is not jointly concave in all three parameters. Therefore, the breaking-rope method cannot be claimed optimal in the scenario considered in this chapter.

Figure 4.6 shows the lower and upper bounds of the optimal policy. To find the lower bound of the total throughput, we plug our solution into the original equation (4.3). On the other hand, plugging the optimal solution back into (4.9), we can find the upper bound for the optimal policy. The upper and lower bounds provide a potential range for the optimal policy. We evaluate the performance by the total throughput of the system, which is depicted as a function of the number of transmission blocks N in the figure. The arrival energy has a uniform distribution in the interval $[0, E_{max}]$

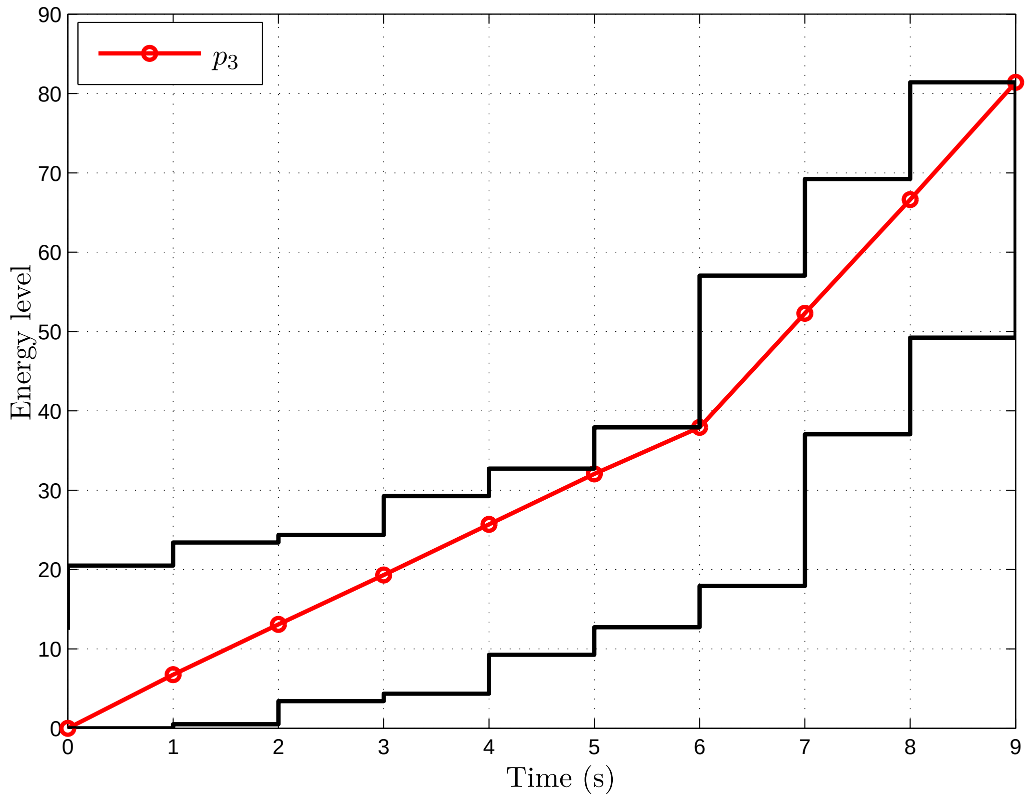

Figure 4.5: Depletion curve of the Relay.

with $E_{max} = 10$. Through Algorithm 2, the optimum polices $\mathbf{p_1}$, $\mathbf{p_2}$ and $\mathbf{p_3}$ are obtained. Moreover, we apply the breaking-rope method to solve the optimization problem in such a case and plug the result back to (4.9). The performance is also depicted in Figure 4.6 for comparison. As can be seen from this figure, when the number of transmission blocks N is equal to 10, our solution can transmit about 13 bits compared with 16 bits of the upper bound. Hence, the maximum loss of performance is $(16-13)/16 = 18.75\%$. As for $N = 20$, the upper bound is approximately 6 bits higher than the lower bound and hence the loss of performance is roughly $6/33 = 18.18\%$. However, as a suboptimal method, breaking-rope transmits almost 1 bit less than our

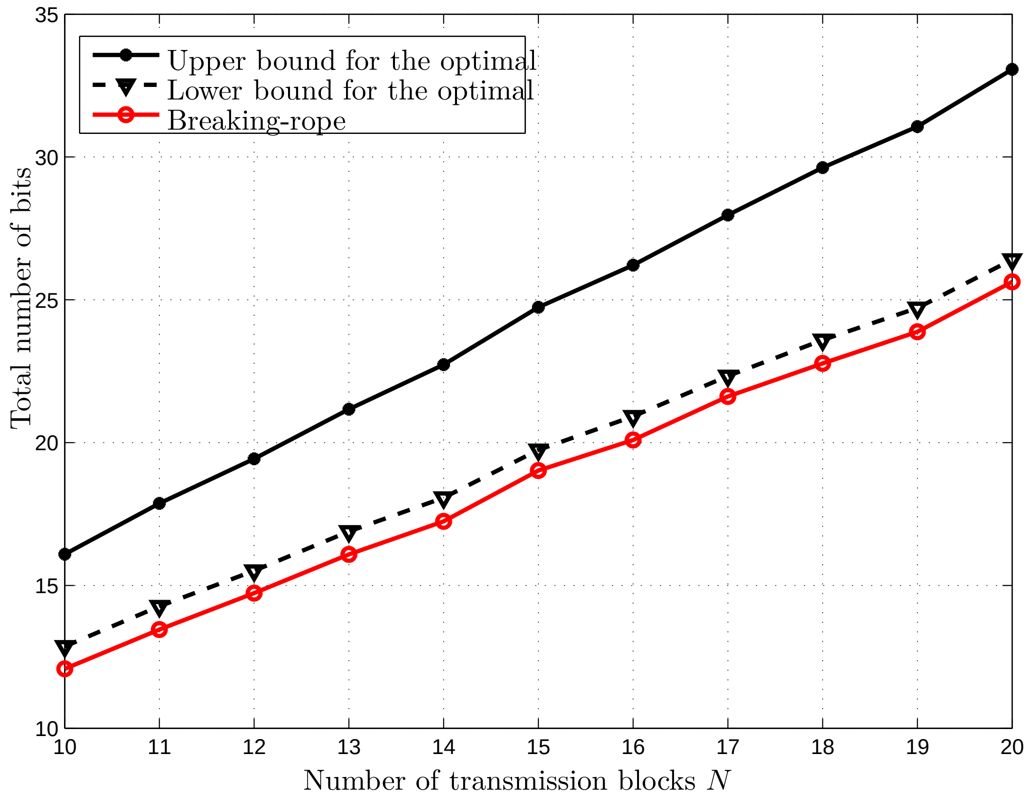

Figure 4.6: Total transmission data versus number of blocks for $E_{max,j} = 10$.

solution throughout the case.

A similar Figure 4.7 is plotted in a case where the total throughput is a function of the maximum battery capacity E_{max}. In such a case, the maximum value of the arrival energy changes with E_{max}. As shown in the Figure 4.7, when the maximum battery capacity is relatively small, i.e., $E_{max} = 1$, the gap between the upper and lower bounds is less than 0.5 bit, the loss of performance is nearly $0.5/2 = 25\%$ and the breaking-rope method is extremely close to the lower bound. When the battery capacity can store 10 energy units at the most, i.e., $E_{max} = 10$, our solution can transmit 13 bits compared with about 16 bits in the best-case scenario, in which the

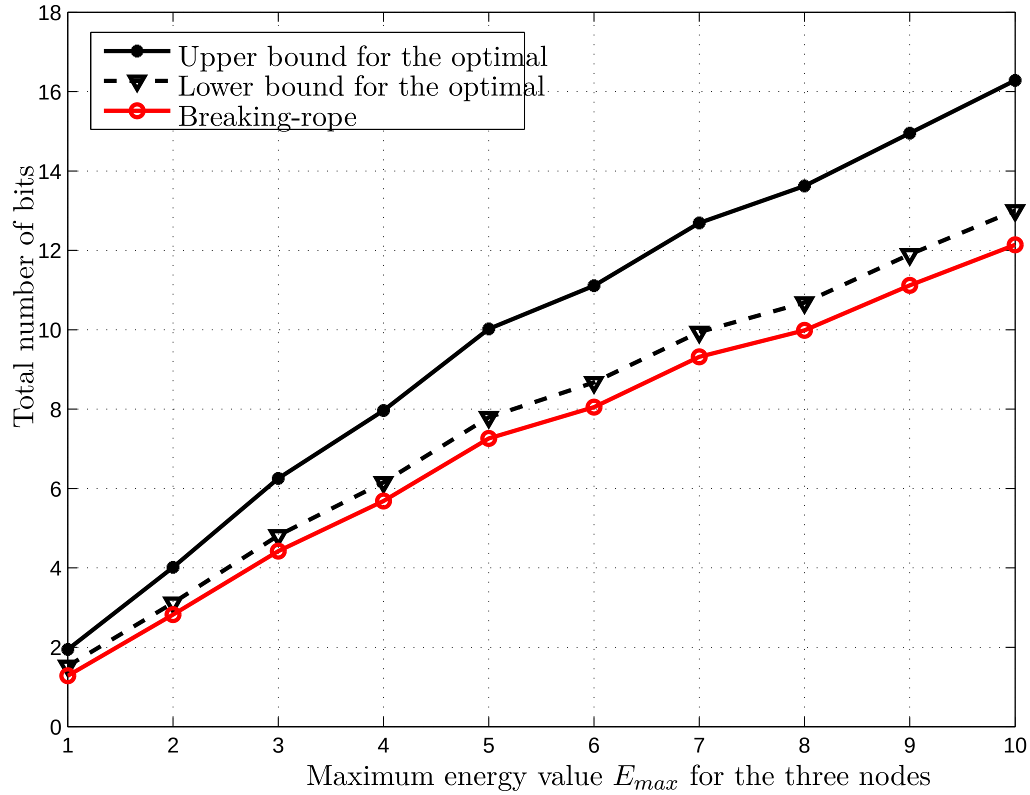

Figure 4.7: Total transmission data versus maximum arrival energy for $N = 10$.

performance is 18.75% worse than the upper bound.

4.4 Summary

In this chapter, we studied the problem of optimal power allocation to maximize the total throughput of an EH two-way AF relay network with three EH nodes. At first, we showed that the objective function is not concave in the optimization parameters and hence it may not be amenable to a computationally efficient solution. However, we relax the function and turn to maximize the upper bound of the total throughput in the best-case. By exploiting the biconvexity property of the relaxed upper bound function, this optimization problem was decomposed into three convex sub-problems. We then introduced the ACS algorithm to solve the sub-problems alternatively. Through computer simulations, the optimal solution obtained by our algorithm was shown. In addition, by plugging our solution back into the original equation (4.3) and the relaxed upper bound equation (4.9), the lower and upper bounds of the optimal policy can be obtained, respectively. These two bounds serve only as a comparison purpose for further study. It was shown that the results obtained by the ACS algorithm are close to the performance of the best-case scenario and outperform the breaking-rope method.

Chapter 5

Conclusion and Future work

5.1 Conclusion

In this thesis, we studied the problem of maximizing the total number of bits energy in a two-way relay EH system in an off-line setting. Such a throughput maximization problem is considered in two cases: 1) only the relay is an EH node, and 2) both transceivers and the relay are EH nodes. The problem is subject to the energy and battery constraints and solved by optimizing the transmitting power of EH node(s).

In the first case, we show that the objective function in our optimization problem is concave in the relay's transmitting power. We then address several properties of the optimal energy allocation policy based on the characteristic of the objective function and exploit the breaking-rope method to solve the problem. We further develop a novel algorithm to realize the breaking-rope method. In the simulation section, the results of the proposed method is compared with other convex optimization solvers, such as CVX and `Fmincon`. In addition, the properties of the optimal solution is shown in the figure through computer simulations.

In the second case, the throughput maximizing problem in the system of three EH nodes is different from the previous. We first show that the objective function is no longer concave in the three optimization parameter vectors which are the transmitting power of three EH nodes, and hence, may not be amenable to a computationally efficient solution. Hence, we have to simplify the objective function to overcome the difficulty in solving the original problem. By relaxing the problem, we aim to find the upper bound of the total throughput. It is shown that the revised function is concave in one parameter when other two parameters are fixed. Thus, the optimal solution can be obtained by using the iterative Alternate Convex Search method. The result of the proposed method addresses the upper bound of the optimal policy. Through computer simulation, we show that our solution performs closely to the best-case. Moreover, the breaking-rope method is evaluated as a sub-optimal method and defeated by our solution.

5.2 Future work

In this thesis, the throughput maximization for EH two-way relay networks is studied. This work can be further investigated in several directions as listed below:

- Deriving the optimal on-line power allocation in a two-way relay system consisting of three EH nodes.
- Deriving the optimal off-line and on-line power allocations in a two-way relay

system consisting of three EH nodes with imperfect battery storages.

- Deriving the optimal power allocation in a two-way relay system with multiple EH relays.

- Deriving the optimal power allocation in a two-way relay MIMO system where all the nodes are powered up by EH devices.

Bibliography

[1] S. Sudevalayam and P. Kulkarni, "Energy harvesting sensor nodes: Survey and implications," *Communications Surveys Tutorials, IEEE*, vol. 13, pp. 443–461, Third 2011.

[2] T. Starner, "Human-powered wearable computing," *IBM Systems Journal*, vol. 35, no. 3.4, pp. 618–629, 1996.

[3] D. Pimentel and P. Musilek, "Power management with energy harvesting devices," in *Electrical and Computer Engineering (CCECE), 2010 23rd Canadian Conference on*, pp. 1–4, May 2010.

[4] T. Voss, V. Subbian, and F. Beyette, "Feasibility of energy harvesting techniques for wearable medical devices," in *Engineering in Medicine and Biology Society (EMBC), 2014 36th Annual International Conference of the IEEE*, pp. 626–629, Aug 2014.

[5] S. Priya and D. J. Inman, *Energy harvesting technologies*, vol. 21. Springer, 2009.

[6] S. Chalasani and J. Conrad, "A survey of energy harvesting sources for embedded systems," in *Southeastcon, 2008. IEEE*, pp. 442–447, April 2008.

[7] X. Lu, P. Wang, D. Niyato, D. I. Kim, and Z. Han, “Wireless networks with rf energy harvesting: A contemporary survey,” *Communications Surveys Tutorials, IEEE*, vol. 17, pp. 757–789, Secondquarter 2015.

[8] M. Chang, M. Dong, and S. ShahbazPanahi, “Joint pairing and power allocation optimization in multichannel mabc-based two-way relaying,” in *Signal Processing Advances in Wireless Communications (SPAWC), 2014 IEEE 15th International Workshop on*, pp. 314–318, June 2014.

[9] A. F. Molisch, *Wireless communications*. John Wiley & Sons, 2007.

[10] S. Talwar, Y. Jing, and S. ShahbazPanahi, “Joint relay selection and power allocation for two-way relay networks,” *Signal Processing Letters, IEEE*, vol. 18, pp. 91–94, Feb 2011.

[11] H. Q. Ngo, T. Quek, and H. Shin, “Amplify-and-forward two-way relay networks: Error exponents and resource allocation,” *Communications, IEEE Transactions on*, vol. 58, pp. 2653–2666, September 2010.

[12] S. J. Kim, N. Devroye, P. Mitran, and V. Tarokh, “Comparison of bi-directional relaying protocols,” in *Sarnoff Symposium, 2008 IEEE*, pp. 1–5, April 2008.

[13] B. Varan and A. Yener, “The energy harvesting two-way decode-and-forward relay channel with stochastic data arrivals,” in *Global Conference on Signal and Information Processing (GlobalSIP), 2013 IEEE*, pp. 371–374, Dec 2013.

[14] I. Ahmed, A. Ikhlef, D. Ng, and R. Schober, “Optimal resource allocation for energy harvesting two-way relay systems with channel uncertainty,” in *Global Con-*

ference on Signal and Information Processing (GlobalSIP), 2013 IEEE, pp. 345–348, Dec 2013.

[15] K. Tutuncuoglu, B. Varan, and A. Yener, “Optimum transmission policies for energy harvesting two-way relay channels,” in *Communications Workshops (ICC), 2013 IEEE International Conference on*, pp. 586–590, June 2013.

[16] K. Tutuncuoglu, B. Varan, and A. Yener, “Throughput maximization for two-way relay channels with energy harvesting nodes: The impact of relaying strategies,” *Communications, IEEE Transactions on*, vol. 63, pp. 2081–2093, June 2015.

[17] E. K. Chong and S. H. Zak, *An introduction to optimization*, vol. 76. John Wiley & Sons, 2013.

[18] S. Boyd and L. Vandenberghe, *Convex optimization*. Cambridge university press, 2004.

[19] O. Ozel and S. Ulukus, “Information-theoretic analysis of an energy harvesting communication system,” in *Personal, Indoor and Mobile Radio Communications Workshops (PIMRC Workshops), 2010 IEEE 21st International Symposium on*, pp. 330–335, Sept 2010.

[20] K. Tutuncuoglu and A. Yener, “Optimum transmission policies for battery limited energy harvesting nodes,” *Wireless Communications, IEEE Transactions on*, vol. 11, pp. 1180–1189, March 2012.

[21] B. Varan and A. Yener, "Two-hop networks with energy harvesting: The (non-)impact of buffer size," in *Global Conference on Signal and Information Processing (GlobalSIP), 2013 IEEE*, pp. 399–402, Dec 2013.

[22] J. Yang and S. Ulukus, "Optimal packet scheduling in an energy harvesting communication system," *Communications, IEEE Transactions on*, vol. 60, pp. 220–230, January 2012.

[23] O. Ozel, K. Tutuncuoglu, J. Yang, S. Ulukus, and A. Yener, "Transmission with energy harvesting nodes in fading wireless channels: Optimal policies," *Selected Areas in Communications, IEEE Journal on*, vol. 29, pp. 1732–1743, September 2011.

[24] M. Zafer and E. Modiano, "A calculus approach to energy-efficient data transmission with quality-of-service constraints," *Networking, IEEE/ACM Transactions on*, vol. 17, pp. 898–911, June 2009.

[25] Y. Luo, J. Zhang, and K. Letaief, "Training optimization for energy harvesting communication systems," in *Global Communications Conference (GLOBECOM), 2012 IEEE*, pp. 3365–3370, Dec 2012.

[26] C. K. Ho and R. Zhang, "Optimal energy allocation for wireless communications with energy harvesting constraints," *Signal Processing, IEEE Transactions on*, vol. 60, pp. 4808–4818, Sept 2012.

[27] Y. Luo, J. Zhang, and K. Letaief, "Optimal scheduling and power allocation for two-hop energy harvesting communication systems," *Wireless Communications, IEEE Transactions on*, vol. 12, pp. 4729–4741, September 2013.

[28] K. Tutuncuoglu and A. Yener, "Transmission policies for asymmetric interference channels with energy harvesting nodes," in *Computational Advances in Multi-Sensor Adaptive Processing (CAMSAP), 2011 4th IEEE International Workshop on*, pp. 197–200, Dec 2011.

[29] K. Tutuncuoglu and A. Yener, "Optimal power control for energy harvesting transmitters in an interference channel," in *Signals, Systems and Computers (ASILOMAR), 2011 Conference Record of the Forty Fifth Asilomar Conference on*, pp. 378–382, Nov 2011.

[30] K. Tutuncuoglu and A. Yener, "Communicating with energy harvesting transmitters and receivers," in *Information Theory and Applications Workshop (ITA), 2012*, pp. 240–245, Feb 2012.

[31] O. Orhan and E. Erkip, "Optimal transmission policies for energy harvesting two-hop networks," in *Information Sciences and Systems (CISS), 2012 46th Annual Conference on*, pp. 1–6, March 2012.

[32] D. Gunduz and B. Devillers, "Two-hop communication with energy harvesting," in *Computational Advances in Multi-Sensor Adaptive Processing (CAMSAP), 2011 4th IEEE International Workshop on*, pp. 201–204, Dec 2011.

[33] A. Minasian, R. Adve, and S. ShahbazPanahi, "Optimal resource allocation in energy harvesting amplify-and-forward relay networks," in *Global Conference on Signal and Information Processing (GlobalSIP), 2013 IEEE*, pp. 363–366, Dec 2013.

[34] O. Orhan and E. Erkip, "Energy harvesting two-hop networks: Optimal policies for the multi-energy arrival case," in *Sarnoff Symposium (SARNOFF), 2012 35th IEEE*, pp. 1–6, May 2012.

[35] I. Ahmed, A. Ikhlef, R. Schober, and R. Mallik, "Joint power allocation and relay selection in energy harvesting af relay systems," *Wireless Communications Letters, IEEE*, vol. 2, pp. 239–242, April 2013.

[36] A. Minasian, S. ShahbazPanahi, and R. Adve, "Energy harvesting cooperative communication systems," *Wireless Communications, IEEE Transactions on*, vol. 13, pp. 6118–6131, Nov 2014.

[37] C. Huang, R. Zhang, and S. Cui, "Throughput maximization for the gaussian relay channel with energy harvesting constraints," *Selected Areas in Communications, IEEE Journal on*, vol. 31, pp. 1469–1479, August 2013.

[38] K. Tutuncuoglu, B. Varan, and A. Yener, "Energy harvesting two-way half-duplex relay channel with decode-and-forward relaying: Optimum power policies," in *Digital Signal Processing (DSP), 2013 18th International Conference on*, pp. 1–6, July 2013.

[39] J. Xu and R. Zhang, "Throughput optimal policies for energy harvesting wireless transmitters with non-ideal circuit power," *Selected Areas in Communications, IEEE Journal on*, vol. 32, pp. 322–332, February 2014.

[40] B. Devillers and D. Gunduz, "A general framework for the optimization of energy harvesting communication systems with battery imperfections," *Communications and Networks, Journal of*, vol. 14, pp. 130–139, April 2012.

[41] K. Tutuncuoglu and A. Yener, "Energy harvesting broadcast channel with inefficient energy storage," in *Signals, Systems and Computers (ASILOMAR), 2012 Conference Record of the Forty Sixth Asilomar Conference on*, pp. 53–57, Nov 2012.

[42] K. Tutuncuoglu, A. Yener, and S. Ulukus, "Optimum policies for an energy harvesting transmitter under energy storage losses," *Selected Areas in Communications, IEEE Journal on*, vol. 33, pp. 467–481, March 2015.

[43] K. Tutuncuoglu and A. Yener, "The energy harvesting multiple access channel with energy storage losses," in *Information Theory Workshop (ITW), 2012 IEEE*, pp. 94–98, Sept 2012.

[44] J. Yang and S. Ulukus, "Transmission completion time minimization in an energy harvesting system," in *Information Sciences and Systems (CISS), 2010 44th Annual Conference on*, pp. 1–6, March 2010.

[45] J. Gorski, F. Pfeuffer, and K. Klamroth, "Biconvex sets and optimization with biconvex functions: a survey and extensions," *Mathematical Methods of Operations Research*, vol. 66, no. 3, pp. 373–407, 2007.